IKs potentiation by ML277 is a novel cardioprotective intervention

Sean Brennan[1#], Abrar IM Alnaimi[1#], Lauren R McGuinness[1], Muhammad IM Abdelaziz[1], Robert A McKenzie[2], Sophie Draycott[2], Jacob Whitmore[1], Parveen Sharma[1] & Richard D Rainbow[1*]

[1]Department of Cardiovascular and Metabolic Medicine & Liverpool Centre for Cardiovascular Sciences, Institute of Life Course and Medical Sciences, University of Liverpool, L69 3GE, UK

[2]Department of Cardiovascular Sciences, College of Life Sciences, University of Leicester, LE1 7RH, UK

[#]These authors contributed equally to this work

*Corresponding Author: Richard Rainbow

Email: richard.rainbow@liverpool.ac.uk

Author Contributions: All work was carried out at the Universities of Liverpool or Leicester in RDR's laboratory.

SB: Contributed to experimental design, acquired, analysed and interpreted the data. Drafted the manuscript.

AIMA: Contributed to experimental design, acquired, analysed and interpreted the data.

LRM: Acquired, analysed and interpreted the data and helped with manuscript revision

MIMA, Acquired, analysed and interpreted the data.

RAM: Acquired, analysed and interpreted the data

SD: Acquired, analysed and interpreted the data

JATW: Acquired, analysed and interpreted the data.

PS: Conception and design of the work, critically appraised and revised the manuscript.

RDR: Conception and design of the work. Acquired, analysed and interpreted data and critically appraised and revised the manuscript.

Competing Interest Statement:

There are no competing interests to disclose.

Classification:

Biological Sciences/Pharmacology

Keywords: Slowly activating voltage-gated potassium current (IKs), Cardioprotection, KCNQ1 (Kv7.1)/KCNE1, ischemic protection, myocardial infarction,

Abstract

Cardiovascular disease is thought to account for nearly a third of deaths worldwide, with ischemic heart disease, including acute coronary syndromes such as myocardial infarction, accounting for 1.7 million deaths per year. There is a clear need for interventions to impart cardioprotection against ischemia. Here, we show that the IKs current potentiator ML277 imparts cardioprotection against ischemia in cellular and whole heart models by modulating the action potential duration. In three different metabolic inhibition and reperfusion models, an increased contractile recovery and cell survival was observed with ML277, indicative of protection. Finally, ML277 reduced infarct size in an *ex vivo* Langendorff coronary ligation model, including if only applied on reperfusion. In conclusion, potentiation of the IKs current with ML277 imparted a cardioprotection that was equivalent to the protection reported previously by ischemic preconditioning. These data suggest that IKs potentiation may be therapeutically useful in acute coronary syndromes.

.

Significance Statement

The heart has an intrinsic ability to protect itself from some damage during acute coronary syndromes, however, activating this cardioprotection in man has proven difficult to translate to the clinic. Here we show that this protection can be mimicked by activation of one the repolarization currents in the heart, IKs. Potentiation of this current may well represent a novel therapeutic target in reducing infarct size in acute coronary syndromes.

Main Text

Introduction

Cardioprotection is a term that can be applied to several scenarios that protect the myocardium from damage but is most commonly used in the context of ischemia. Since Murry *et al*'s seminal 1986 publication demonstrating a protective effect in canine hearts imparted by a short period of ischemia prior to the main insult(1), the means of activating this protection clinically has been the subject of many investigations. In the nearly 40 years following this ground-breaking discovery, there have been a myriad of mechanisms hypothesized, however the clinical translation of these has proven difficult.

Our, and others, previous findings demonstrate that cardioprotection, imparted by several mechanisms that activate a PKC-dependent process, such as ischemic preconditioning (IPC), adenosine and pharmacological interventions, cause modulation of the action potential and reduced consumption of ATP during ischemic conditions, leading to improved Ca^{2+} handling (2-7). From these findings, it was hypothesized action potential shortening, by selectively modulating an appropriate ion channel, would mimic the action potential shortening triggered by activation of the RISK pathways therefore reproducing the cardioprotective outcome pharmacologically.

Kv7.1 (KCNQ1) together with KCNE1 (previously referred to as MinK) from the complex that carries the IKs current in the heart and are encoded by the *KCNQ1* and *KCNE1* genes, respectively. The stoichiometry of KCNQ1 and KCNE1 in the IKs complex has been heavily debated, however, reports have demonstrated mammalian cells contain two KCNE1 accessory subunits per channel complex (8). IKs is responsible for the slow component of the delayed rectifier K^+ currents and plays a role in repolarisation on the cardiac membrane potential following an action potential. The key role for IKs is underscored by various loss-of-function mutations causing long QT syndrome which decreased the currents amplitude and consequently prolongs the cardiomyocyte APD (9).

ML277 is a potent Kv7.1 channel potentiator (10, 11) and selective against other KCNQ channels and other cardiac ion channels including hERG, Nav1.5, and Cav1.2 (12). ML277 preferentially activates Kv7.1 in the absence of the KCNE1 β-subunit and is less effective at potentiating KCNQ1 when saturated with KCNE1 (4:4 ratio). ML277 has been shown to potentiate native IKs in guinea pig and canine ventricular myocytes and human (iPSC)-derived cardiomyocytes (12, 13). The ability of ML277 to abolish calcium transient and action potential alternans in rabbit atrial myocytes (14), and reverse decreased IKs current to partially restore action potential duration in LQT1 patient-derived human iPSC-cardiomyocytes (15), has led others to report IKs may have therapeutic value as an anti-arrhythmic target.

Here we demonstrate that ML277 can impart cardioprotection in cellular and whole-heart models of acute coronary syndromes, via a mechanism involving action potential shortening and reduced Ca^{2+} accumulation, similar to established cardioprotective pathways. These data suggest that IKs potentiation can confer cardioprotection and may be beneficial in acute coronary syndromes.

Results

Rat ventricular cardiomyocytes express an ML277-sensitive current

To investigate whether treatment with ML277 was protective in isolated cardiomyocytes, an initial investigation was carried to confirm the presence of an ML277-sensitive current in rat cardiomyocytes. Voltage-gated K^+ currents were activated using a whole-cell protocol, depolarizing from -60 mV to 60 mV in 20 mV steps for 6 s, followed by a step to -30 mV for 1 s. Cells were then perfused with Tyrode's solution containing 1 μM ML277 for 5 min, with the protocol repeated twice. Figure 1A shows the final 200 ms of the 6 s depolarization in the absence, and presence of 1 μM ML277, showing a larger current in the ML277 trace in both the voltage-steps and in the tail currents. As ML277 is far less effective on channels containing 4 KCNE1 subunits (12), these data imply native IKs channels in rat ventricular myocytes, as previously reported in canine and guinea pig (13), are not saturated with KCNE1. These data are similar to those recorded in HEK293 cells transiently transfected with KCNQ1/KCNE1 subunits (Figure S1), where there was an increase in the whole-cell current. In both cardiomyocytes (Figure 1A and B) and in HEK293 cells (Figure S1D and E), there was a leftward shift in the activation curve (-6 ± 2 mV in the absence, and -29 ± 2 mV in the presence of ML277), consistent with previous reports of the effects of ML277 on the IKs complex (12, 13). In both cardiomyocytes and HEK293 cells, there was a significant increase in the current recorded at 20 mV (Figure 1D, and Figure S1C respectively). Potentiation of a delayed rectifier current in rat ventricular myocytes would be expected to cause an action potential shortening by increasing the repolarizing K^+ currents. To investigate this, action potential recordings were carried out using current-clamp recording. In these experiments, perfusion with 1 μM ML277, caused significant shortening of the action potential duration to 90% repolarized (APD_{90}) (Figure 1 E – G), comparable to the shortening reported in rabbit atrial action potentials (14). Coupled to this, the calcium transients, as measured using the ratiometric indicator Fura-2, showed a reduced amplitude and reduced area under the curve in the presence of ML277 (Figure 1 H – J). For a more detailed analysis of the kinetics of the calcium transients, cells loaded with Fluo-4 were used and the transient duration, amplitude and area under the curve were analyzed. These data showed a significant blunting of the transients, with an increased rate of return from peak to baseline (Figure S2A-F). Contractile function of cardiomyocytes in the presence of 1 μM ML277 was also assessed using video-edge detection, demonstrating a significant reduction in contractile amplitude and area under the curve (Figure S2G-L). Together, these data demonstrate that there is an ML277-sensitive current expressed in rat ventricular cardiomyocytes that is able to modulate the action potential duration and the calcium accumulation during each contractile cycle.

ML277 only potentiated the voltage-gated K^+ channel component of the cardiomyocytes currents, having no significant effect on calcium or IK_1 currents or hERG stably expressed in HEK293 cells (Figure S3 & S4), analogous to previous reports of ML277 not altering other cardiac currents (12-14). Increasing ML277 concentration to 3 μM had no further potentiating effect on the shortening of the APD (Figure S4), suggesting that ML277 has a limit to its effect on APD shortening. Conversely, the IKs channel blocker, JNJ303, inhibited IKs current reversibly, and did not affect other currents greater than the run down seen in these experiments (Figure S5). To assess the potential translation of these data from rat to humans, the increase of IKs current demonstrated in cardiomyocytes (Figure 1) and in HEK 293 cells (Figure S1) was modelled in a computer

simulation used in investing the outcome of CiPA screening, O'Hara-Rudy CiPA v1.0 (2017) model (16). In human epicardial, myocardial and endocardial models' of IKs potentiation, achieved by shifting the activation curve leftwards by 30 mV, showed action potential shortening, an increase in IKs current and a decrease in the simulated intracellular calcium transient amplitude in all cell types modelled (Figure S6).

Treatment of cardiomyocytes with ML277 has a cardioprotective effect:

Comparable to the effect of ML277 on action potential duration and calcium transients (Figure 1), cardiomyocytes exposed to well-established cardioprotective stimuli also display a shorter cardiac action potential and reduced Ca^{2+}-load during each contractile cycle (2, 17). These similarities led to the hypothesis that ML277 imparts cardioprotection against metabolic inhibition through shortening the action potential duration and improved calcium handling.

Cardiomyocytes were exposed to a metabolic inhibition and washout protocol that has been used in our (2, 17-20), and others (5, 21-27), previous publications to assess cardioprotection and toxicity. Figure 2A shows the mean time course of the percentage of contractile cardiomyocytes in control conditions, ML277 (0.1, 0.3, 1, or 3 μM), and with the selective IKs blocker JNJ303 (1 μM) (28). Consistent with established cardioprotective stimuli, ML277 caused a delay in the time to contractile failure (Figure 2B), an increased contractile recovery (Figure 2C) and an increase in cell survival (Figure 2D). These effects were also replicated in an ischemic buffer as used previously in our group (2), and in a modified metabolic poison solution using sodium azide (Figure S7A and B). Similar effects were observed in guinea pig cardiomyocytes, where both contractile recovery and cell survival increased in a concentration-dependent manner (Figure S7C and D). Finally, JNJ303, demonstrated a cardiotoxic effect by causing a significant reduction in the time to contractile failure (Figure 2B) and a decrease in the contractile recovery (Figure 2C) and cell survival (Figure 2D).

As further evidence of a cardioprotective effect of ML277 in isolated rat cardiomyocytes, the accumulation of intracellular Ca^{2+} (measured using Fluo-4), and mitochondrial depolarization (measured using TMRM), were measured. The Fluo-4 fluorescence peak induced by metabolic inhibition was smaller in the presence of 1 μM ML277, and the initiation of this increase was delayed (Figure S8A – C) (2). The mean time to mitochondrial depolarization, was not different between the treated and non-treated groups, however the peak amplitude of TMRM signal was significantly lower in the ML277-treated group (Figure S6D – F). These data agree with our previous findings in cardioprotected cells (2). These findings demonstrate that ML277 has a protective effect on freshly isolated rat and guinea pig cardiomyocytes, as evidenced by improved contractile recovery, calcium handling and cell survival plus reduced cell death and mitochondrial depolarization.

ML277 is cardioprotective in a rat *ex vivo* whole heart coronary ligation model

To assess whether ML277 can act as a cardioprotectant in the whole heart, *ex vivo* left anterior descending (LAD) coronary artery occlusion was performed on a Langendorff system. ML277 reduced infarct size at concentrations greater than 300 nM (Figure 3A and B), consistent with the cellular metabolic inhibition data (Figure 2 and Supplementary Figures 5 and 6). Furthermore, IKs

blocker JNJ303 increased infarct size, consistent with the cellular metabolic inhibition data (Figure 3). Clinically useful therapeutics would most likely be administered either once ischemia was established or upon reperfusion. To model the clinical scenario, ML277 was applied either 20 minutes into the coronary ligation, or on reperfusion only. In these hearts, the infarct size was significantly reduced compared with control conditions (Figure 3C). These data show that ML277 imparted cardioprotection against ischemia and reperfusion injury to the whole heart.

Discussion

In this study, we demonstrate that the KCNQ1 activating compound, ML277, has a protective effect on cardiomyocytes, and can reduce infarct size in a whole heart *ex vivo* model using coronary ligation. Our data show the activation of a delayed rectifier current in rat ventricular myocytes increases the current in the repolarizing phase of the rat ventricular action potential causing a significant APD_{90} shortening. The intracellular Ca^{2+} transients recorded from isolated cardiomyocytes show a reduced amplitude and area under the curve, suggesting reduced Ca^{2+} accumulation during each contractile cycle, thus reducing the ATP required to restore diastolic Ca^{2+} levels (Figure 4). This reduced ATP consumption allows cells to maintain Ca^{2+} homeostasis for longer during metabolic inhibition and survive reperfusion more readily. We have previously demonstrated such time-dependence to the reperfusion using this metabolic poison with ischemic preconditioned cells, or treatment with adenosine, diazoxide and pinacidil; all well-established cardioprotective interventions (2). Modelling the effects of IKs potentiation with the O'Hara-Rudy CiPA v1.0 (2017) model also showed that a marked shortening of the human APD corresponded with a reduced Ca^{2+} transient amplitude.

The use of direct ion channel modulation to impart cardioprotection is not unique. Pinacidil, amongst other ATP-sensitive potassium (K_{ATP}) channel modulators, has been shown to have a cardioprotective effect. Activation of K_{ATP} channels is thought to be protective by limiting cellular excitability and so reducing ATP consumption, however care should be taken with this as the known cardiac K_{ATP} complex, Kir6.2/SUR2A, is an abundantly expressed protein in the heart and its activation can cause significant cardiac action potential shortening, and subsequent complete failure. Gain of function mutations of the cardiac K_{ATP} channel complex has been shown to cause short-QT syndrome and is proarrhythmic.

The established cardioprotection imparted by K_{ATP} channel activation demonstrates that direct increase in outward K^+ efflux and subsequent action potential shortening can be cardioprotective, thus it is plausible that IKs potentiation can be cardioprotective. Further support of the protective effect for IKs can be found in the literature where the contribution of IKs to repolarization during ischaemia is increased, and in these conditions IKs blockade with L-768,673 causes an increase in ventricular arrhythmias (29). This reported anti-arrhythmic effect of IKs potentiation with ML277 is also a potential important therapeutic area where increasing the rate of repolarization, as our data suggests is occurring, could reduce the potential for early and delayed after-depolarizations triggered by high intracellular Ca^{2+} accumulations. A further consideration is the potential use of IKs as a drug-target in certain long-QT syndromes, such as LQT-1, where the presence of some functional IKs current could be potentiated to limit the incidence of fatal ventricular arrhythmias.

In contrast to these findings, it has reported that pan-Kv7 blockers improve infarct size in isolated rat hearts against ischemia reperfusion injury (30), but at an estimated concentration of 1 µM, the pan-Kv7 blocker XE991 did not improve infarct size during *in vivo* experiments (31). Although 1 µM XE991 does block Kv7.1 channels (32), Kv7.1/KCNE1 channels in oocytes display negligible block with 1 µM XE991 and 40% block to 10 µM after a 500-ms depolarizing step (33). It is, therefore, unlikely that the native cardiac IKs complex is susceptible to XE991 block over the duration of the cardiac action potential (<400 ms). Kv4.3, which contributes to the I_{To} current in myocytes (34), is blocked by XE991 with a reported IC50 of 43 ± 7 µM (32). This may explain the reported protective effect of 10 µM XE991 with *in vitro* experiments showing that 10 µM XE991

did not alter the rat atrial action potential duration and caused an approximate 10 ms prolongation in guinea pig (31). Interestingly, the IKs blocker Chromanol 293B appears to increase infarct size by >10 %, but a larger n number was likely required to achieve significance (30).

The use of small molecules to modulate an ion channels activity can raise questions regarding selectivity, however as previously reported no major unspecific action of ML277 in the heart has been described (14). ML277 has been shown to be highly selective against other recombinant cardiac channels hERG, Na1.5 and Cav1.2 and other members of the Kv7 ion channel family (12). In a binding assay panel of 68 GPCRs, ion channels and transporters, 10 µM ML277 was found to bind with only 6 assays conducted (35). The report states functional selectivity may be significantly better than suggested by binding activities and such discrepancies are not uncommon. For example, 10 µM ML277 was shown to have 80% inhibition against the hERG channel in a binding assay, but 30 µM ML277 had no activity against hERG in a functional assay. Our own whole-cell patch-clamp data also demonstrates ML277 does not functionally inhibit hERG at 3 µM. In our assays, ML277 displayed cardioprotection at approximately 300 nM which is close to the drugs reported EC_{50} for IKs. Furthermore, the selective IKs blocker JNJ303, which has no potent effects on the other cardiac ion channels (I_{Na}, I_{Ca}, I_{Kr}, I_{To}, I_{K1}) (36), displayed the opposite effect to ML227 and blocked the protection imparted by ML277. Although off-target effects can never be entirely ruled out, taking into account the known selectivity profile of the drugs used in this study, we conclude the effects observed are due to modulation of IKs.

Gain of function mutations of the IKs complex in the heart are rare and do give rise to short QT syndromes in those affected. Such mutations tend to change the currents properties from a slowly activating to rapidly activating, often by reducing its association with the KCNE1 subunit (37, 38). In comparison, ML277 causes a leftwards shift in the activation curve for IKs as recorded in both ventricular myocytes and the cloned human subunits expressed in HEK293 cells. The current maintains its slowly activating component and does not excessively shorten the $APD_{90,}$ as would be seen in short-QT syndromes. This gives ML277 an advantage over sulphonylurea compounds that activate the K_{ATP} complex as cardioprotective agonists. The cardiac K_{ATP} complex has a Kir6.2 pore that forms a weakly rectifying K^+ channel. This weak rectification property means that once activated, this complex passes K^+ flux at any membrane potential with an increasing hyperpolarizing influence the more depolarized, or further from E_K, the membrane potential becomes. It is entirely plausible that, with significant K_{ATP} complex activation, contractile failure could arise, which does indeed happen during significant periods of ischemia. Pharmacological potentiation of the IKs complex is unlikely to be so damaging to contractile function. Firstly, the effects of IKs on the cardiac action potential at rest are limited. Indeed, long-QT syndrome type-I (KCNQ1 loss of function mutations) is often subclinical and is only detected after a cardiac event, or through genetic screening. The IKs complex, forming part of the delayed rectifier component of currents, is not a dominant repolarizing current until significant sympathetic drive. Additionally, this current is already active in cardiac cells, with ML277 potentiating that current. Opening of the K_{ATP} complex, however, is a pathophysiological event, usually associated with significant metabolic stress. Finally, the IKs complex carries a voltage-dependent current that is only activated on depolarization, therefore potentiating this current will speed up repolarization and so is unlikely to prevent depolarization, in contrast to the Kir6.2/SUR2A K_{ATP} current. Our data, supplementary Figure 4, shows that increasing ML277 to 3 µM did not cause an increase in the effectiveness of the ADP shortening. These data suggest a “ceiling” to the effect that IKs potentiation has on APD in the context of pharmacological activation. This is potentially due to

the slow kinetics of the IKs current, where even with potentiation by ML277, the current still develops too slowly to cause a shortening that would be pro-arrhythmic. This would be an important consideration from a safety aspect where excessive shortening would not only be pro-arrhythmic, but also could significantly impair cardiac output to the detriment of the patient.

The mechanisms by which cardioprotection is imparted are complex and have been referred to as Reperfusion Injury Salvage Kinase (RISK) pathways, which often involves the short-term activation of kinases (39-42). It has been suggested to comprise two parallel pathways, PI3K-Akt and MEK1-ERK1/2, being activated (42). Many of these potential pathways converge on PKC activation, particularly PKCε and PKCδ in the early and second windows of protection, respectively (43-45)) (27, 44)). The activators of this pathway can be varied, and can occur via metabolites released in stress conditions (e.g. adenosine (2, 46, 47)) or from endogenous receptor agonists (e.g. bradykinin and opioids (48-50)) but often occur in during a hypoxic state. In metabolically compromised tissue, these pathways may be difficult to modulate given the potentially low ATP availability for phosphorylation events which could render the pathway non-functional. Similarly, it is plausible that ATP and PIP_2 depletion experienced during ischemia may underlie the reported downregulation of IKs, contributing to the proarrhythmic mechanism associated with poor outcomes from myocardial infarction (29). The administration of ML277, or an alternative IKs potentiator, could overcome this loss of expression so reducing proarrhythmicity, in addition to protecting against ischemic injury. We suggest IKs potentiation could therefore bypass the metabolic compromise or stress responses seen during ischemia, may result in better clinical translation of a cardioprotective intervention.

In conclusion, we have presented data to demonstrate that ML277 has the potential to be a cardioprotective agonist that acts directly on a channel complex to reduce Ca^{2+} loading during ischemia and therefore preserve ATP for longer. This provides a mechanism by which the cell can delay, or at least slow, the Ca^{2+} accumulation that occurs with ATP depletion and therefore survive an ischemic insult more readily. The fact that this method of cardioprotection does not rely on the complex intracellular signaling via the RISK pathway, is potentially of benefit given that few cardioprotective interventions with positive pre-clinical data translate to the clinic.

This work demonstrates that in *ex vivo* cellular and whole-heart models of ischemia reperfusion that IK_S potentiation is beneficial. Further work is required to determine if this mechanism is suitable in higher species and whether similar effects can be observed *in vivo*.

Materials and Methods

Cardiomyocyte isolation:

The care and sacrifice of the animals conformed to the requirements of the UK Animals (Scientific Procedures) Act 1986 (2012 amendment). Ethical approval for all experimental procedures was granted by the University of Liverpool/Leicester's Animal Welfare and Ethical Review Body (AWERB_2018_44). Adult male Wistar rats (200 – 300 g) were killed by Schedule 1 procedure of concussion and cervical dislocation. Cell isolations were carried out as previously reported (2, 17, 20). Ischemic preconditioning was carried out on the whole whole-heart on a Langendorff canula using a stop-start perfusion protocol (2, 17, 20). See supplementary methods section for full details.

Electrophysiology:

Patch clamp recordings were carried out using isolated cardiomyocytes in the whole-cell configuration as described previously (2, 17, 20). See supplementary methods for full details.

Metabolic inhibition:

A well-established metabolic inhibition protocol was used to monitor cardiomyocytes contractility and survival. 2 mM cyanide and 1 mM iodoacetic acid were added to a substrate-free metabolic inhibition Tyrode's solution (SFT-MI) (see supplementary information for solution components) and perfused on isolated cardiomyocytes, simulated to contract via 1 Hz stimulation as described previously (2, 17, 20). See supplementary methods for full details.

Fluorescence imaging:

To record calcium transients, cardiomyocytes were loaded with 5 µM Fura-2-AM for 20 minutes at room temperature. Cardiomyocytes were stimulated to contract at 1 Hz using electric field stimulation (EFS) and perfused at 32°C. Data was acquired using Winfluor4.1.6 software (Strathclyde University), with 340 and 380 nm excitation illumination provided by a PTI DeltaRam X monochromator. Emissions were collected using an Andor Zyla4.5 camera at wavelength greater than 520 nm. Images were acquired at a rate of 26 ratios per second.

Ex vivo coronary ligation:

A standard left anterior descending coronary artery ligation model was used to cause an infarct to a Langendorff perfused heart. The artery was ligated for 40 minutes, followed by 3 hours of reperfusion, where infarct was measured using tetrazolium chloride staining, as previously reported (17). See supplementary methods for full details.

Competing interests

No authors have any competing interests to declare.

Data availability

The data that support the findings of this study are available in this manuscript and the Supplementary Material..

Acknowledgments

We acknowledge support from the British Heart Foundation (SB & RDR (PG/16/14/32039 & PG/19/18/34280), and LRM (FS/PhD/21/29165)). This work was also supported by an internal funding scheme funded by the Wellcome Trust Institutional Strategic Support Fund grant (204822/Z/16/Z) and awarded to SB & RDR by the Faculty of Health and Life Sciences, University of Liverpool.

References

1. C. E. Murry, R. B. Jennings, K. A. Reimer, Preconditioning with ischemia: a delay of lethal cell injury in ischemic myocardium. *Circulation* **74**, 1124-1136 (1986).
2. S. Brennan *et al.*, Early opening of sarcolemmal ATP-sensitive potassium channels is not a key step in PKC-mediated cardioprotection. *J Mol Cell Cardiol* **79**, 42-53 (2015).
3. C. Ozcan, M. Palmeri, T. L. Horvath, K. S. Russell, R. R. Russell, 3rd, Role of uncoupling protein 3 in ischemia-reperfusion injury, arrhythmias, and preconditioning. *Am J Physiol Heart Circ Physiol* **304**, H1192-1200 (2013).
4. R. M. Fryer, J. T. Eells, A. K. Hsu, M. M. Henry, G. J. Gross, Ischemic preconditioning in rats: role of mitochondrial K(ATP) channel in preservation of mitochondrial function. *Am J Physiol Heart Circ Physiol* **278**, H305-312 (2000).
5. H. E. Turrell, C. Thaitirarot, H. Crumbie, G. Rodrigo, Remote ischemic preconditioning of cardiomyocytes inhibits the mitochondrial permeability transition pore independently of reduced calcium-loading or sarcKATP channel activation. *Physiol Rep* **2** (2014).
6. L. Lu *et al.*, Metformin prevents ischaemic ventricular fibrillation in metabolically normal pigs. *Diabetologia* **60**, 1550-1558 (2017).
7. R. Macianskiene *et al.*, Mechanism of Action Potential Prolongation During Metabolic Inhibition in the Whole Rabbit Heart. *Front Physiol* **9**, 1077 (2018).
8. L. D. Plant, D. Xiong, H. Dai, S. A. Goldstein, Individual IKs channels at the surface of mammalian cells contain two KCNE1 accessory subunits. *Proc Natl Acad Sci U S A* **111**, E1438-1446 (2014).
9. X. Wu, H. P. Larsson, Insights into Cardiac IKs (KCNQ1/KCNE1) Channels Regulation. *Int J Mol Sci* **21** (2020).
10. M. E. Mattmann *et al.*, Identification of (R)-N-(4-(4-methoxyphenyl)thiazol-2-yl)-1-tosylpiperidine-2-carboxamide, ML277, as a novel, potent and selective K(v)7.1 (KCNQ1) potassium channel activator. *Bioorg Med Chem Lett* **22**, 5936-5941 (2012).
11. K. Willegems *et al.*, Structural and electrophysiological basis for the modulation of KCNQ1 channel currents by ML277. *Nat Commun* **13**, 3760 (2022).
12. H. Yu *et al.*, Dynamic subunit stoichiometry confers a progressive continuum of pharmacological sensitivity by KCNQ potassium channels. *Proc Natl Acad Sci U S A* **110**, 8732-8737 (2013).
13. Y. Xu *et al.*, Probing binding sites and mechanisms of action of an I(Ks) activator by computations and experiments. *Biophys J* **108**, 62-75 (2015).
14. G. Kanaporis, Z. M. Kalik, L. A. Blatter, Action potential shortening rescues atrial calcium alternans. *J Physiol* **597**, 723-740 (2019).
15. D. Ma *et al.*, Characterization of a novel KCNQ1 mutation for type 1 long QT syndrome and assessment of the therapeutic potential of a novel IKs activator using patient-specific induced pluripotent stem cell-derived cardiomyocytes. *Stem Cell Res Ther* **6**, 39 (2015).
16. S. Dutta *et al.*, Optimization of an In silico Cardiac Cell Model for Proarrhythmia Risk Assessment. *Front Physiol* **8**, 616 (2017).
17. S. Brennan *et al.*, A novel form of glycolytic metabolism-dependent cardioprotection revealed by PKCalpha and beta inhibition. *J Physiol* **597**, 4481-4501 (2019).

18. C. L. Lawrence, R. D. Rainbow, N. W. Davies, N. B. Standen, Effect of metabolic inhibition on glimepiride block of native and cloned cardiac sarcolemmal K(ATP) channels. *Br J Pharmacol* **136**, 746-752 (2002).
19. R. D. Rainbow *et al.*, SUR2A C-terminal fragments reduce KATP currents and ischaemic tolerance of rat cardiac myocytes. *J Physiol* **557**, 785-794 (2004).
20. M. W. Sims *et al.*, PKC-mediated toxicity of elevated glucose concentration on cardiomyocyte function. *Am J Physiol Heart Circ Physiol* **307**, H587-597 (2014).
21. D. Hudman, N. B. Standen, Protection from the effects of metabolic inhibition and reperfusion in contracting isolated ventricular myocytes via protein kinase C activation. *J Mol Cell Cardiol* **37**, 579-591 (2004).
22. C. L. Lawrence, B. Billups, G. C. Rodrigo, N. B. Standen, The KATP channel opener diazoxide protects cardiac myocytes during metabolic inhibition without causing mitochondrial depolarization or flavoprotein oxidation. *Br J Pharmacol* **134**, 535-542 (2001).
23. G. C. Rodrigo, N. W. Davies, N. B. Standen, Diazoxide causes early activation of cardiac sarcolemmal KATP channels during metabolic inhibition by an indirect mechanism. *Cardiovasc Res* **61**, 570-579 (2004).
24. G. C. Rodrigo, C. L. Lawrence, N. B. Standen, Dinitrophenol pretreatment of rat ventricular myocytes protects against damage by metabolic inhibition and reperfusion. *J Mol Cell Cardiol* **34**, 555-569 (2002).
25. G. C. Rodrigo, N. J. Samani, Ischemic preconditioning of the whole heart confers protection on subsequently isolated ventricular myocytes. *Am J Physiol Heart Circ Physiol* **294**, H524-531 (2008).
26. G. C. Rodrigo, N. B. Standen, Role of mitochondrial re-energization and Ca2+ influx in reperfusion injury of metabolically inhibited cardiac myocytes. *Cardiovasc Res* **67**, 291-300 (2005).
27. H. E. Turrell, G. C. Rodrigo, R. I. Norman, M. Dickens, N. B. Standen, Phenylephrine preconditioning involves modulation of cardiac sarcolemmal K(ATP) current by PKC delta, AMPK and p38 MAPK. *J Mol Cell Cardiol* **51**, 370-380 (2011).
28. E. Wrobel *et al.*, KCNE1 induces fenestration in the Kv7.1/KCNE1 channel complex that allows for highly specific pharmacological targeting. *Nat Commun* **7**, 12795 (2016).
29. X. Guo *et al.*, IKs protects from ventricular arrhythmia during cardiac ischemia and reperfusion in rabbits by preserving the repolarization reserve. *PLoS One* **7**, e31545 (2012).
30. J. Hansen *et al.*, Impact of Administration Time and Kv7 Subchannels on the Cardioprotective Efficacy of Kv7 Channel Inhibition. *Drug Des Devel Ther* **14**, 2549-2560 (2020).
31. K. K. Corydon *et al.*, Effect of ischemic preconditioning and a Kv7 channel blocker on cardiac ischemia-reperfusion injury in rats. *Eur J Pharmacol* **866**, 172820 (2020).
32. H. S. Wang *et al.*, KCNQ2 and KCNQ3 potassium channel subunits: molecular correlates of the M-channel. *Science* **282**, 1890-1893 (1998).
33. H. S. Wang, B. S. Brown, D. McKinnon, I. S. Cohen, Molecular basis for differential sensitivity of KCNQ and I(Ks) channels to the cognitive enhancer XE991. *Mol Pharmacol* **57**, 1218-1223 (2000).

34. C. E. Molina, J. Heijman, D. Dobrev, Differences in Left Versus Right Ventricular Electrophysiological Properties in Cardiac Dysfunction and Arrhythmogenesis. *Arrhythm Electrophysiol Rev* **5**, 14-19 (2016).
35. L. Z. Yu H, Xu K, Huang X, Long S, Wu M, McManus OB, Le Engers J, Mattmann ME, Engers DW, Le UM, Lindsley CW, Hopkins CR, Li M., Identification of a novel, small molecule activator of KCNQ1 channels. *Probe Reports from the NIH Molecular Libraries Program [Internet].* (2011).
36. R. Towart *et al.*, Blockade of the I(Ks) potassium channel: an overlooked cardiovascular liability in drug safety screening? *J Pharmacol Toxicol Methods* **60**, 1-10 (2009).
37. C. Moreno *et al.*, A new KCNQ1 mutation at the S5 segment that impairs its association with KCNE1 is responsible for short QT syndrome. *Cardiovasc Res* **107**, 613-623 (2015).
38. Y. H. Chen *et al.*, KCNQ1 gain-of-function mutation in familial atrial fibrillation. *Science* **299**, 251-254 (2003).
39. D. J. Hausenloy, D. M. Yellon, Reperfusion injury salvage kinase signalling: taking a RISK for cardioprotection. *Heart Fail Rev* **12**, 217-234 (2007).
40. D. J. Hausenloy, D. M. Yellon, Preconditioning and postconditioning: united at reperfusion. *Pharmacol Ther* **116**, 173-191 (2007).
41. D. J. Hausenloy, A. Tsang, D. M. Yellon, The reperfusion injury salvage kinase pathway: a common target for both ischemic preconditioning and postconditioning. *Trends Cardiovasc Med* **15**, 69-75 (2005).
42. X. Rossello, D. M. Yellon, The RISK pathway and beyond. *Basic Res Cardiol* **113**, 2 (2018).
43. G. R. Budas, D. Mochly-Rosen, Mitochondrial protein kinase Cepsilon (PKCepsilon): emerging role in cardiac protection from ischaemic damage. *Biochem Soc Trans* **35**, 1052-1054 (2007).
44. N. Duquesnes, F. Lezoualc'h, B. Crozatier, PKC-delta and PKC-epsilon: foes of the same family or strangers? *J Mol Cell Cardiol* **51**, 665-673 (2011).
45. T. Miura, HASF, a PKC-epsilon activator with novel features for cardiomyocyte protection. *J Mol Cell Cardiol* **69**, 1-3 (2014).
46. M. V. Cohen, C. P. Baines, J. M. Downey, Ischemic preconditioning: from adenosine receptor to KATP channel. *Annu Rev Physiol* **62**, 79-109 (2000).
47. A. Dana, G. F. Baxter, D. M. Yellon, Delayed or second window preconditioning induced by adenosine A1 receptor activation is independent of early generation of nitric oxide or late induction of inducible nitric oxide synthase. *J Cardiovasc Pharmacol* **38**, 278-287 (2001).
48. T. Minamino, Cardioprotection from ischemia/reperfusion injury: basic and translational research. *Circ J* **76**, 1074-1082 (2012).
49. J. M. Downey, A. M. Davis, M. V. Cohen, Signaling pathways in ischemic preconditioning. *Heart Fail Rev* **12**, 181-188 (2007).
50. P. K. Randhawa, A. S. Jaggi, Opioids in Remote Ischemic Preconditioning-Induced Cardioprotection. *J Cardiovasc Pharmacol Ther* **22**, 112-121 (2017).

Figures and Tables

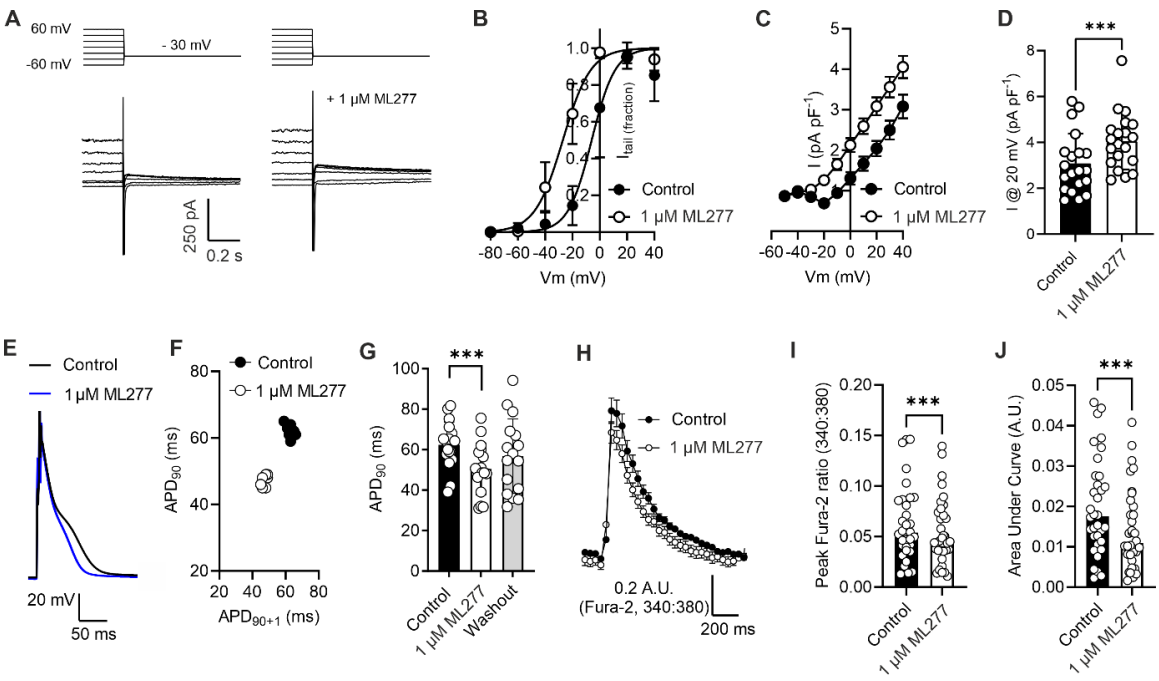

Figure 1.

ML277 activates delayed rectifier K^+ currents to shorten the cardiac action potential duration and reduce the Ca^{2+} transients

(A) Example traces of currents recorded in a rat ventricular myocyte in control conditions and following 5 minutes of perfusion with 1 µM ML277 at the end of a 6 second depolarizing step, back to -30 mV to measure tail currents. **(B)** Tail currents measured at -30 mV normalized to maximum tail current in the absence (control) and presence of 1 µM ML277 (n = 6 cells). Half maximal activation was -6 ± 2 mV in the absence, and -29 ± 2 mV in the presence of ML277. **(C)** Mean current-voltage relationship recorded from the end of a 6 second depolarizing step from a holding potential of -70 mV in the presence and absence of 1 µM ML277. **(D)** Mean peak current amplitude in the absence (control) and presence of 1 µM ML277 (***P<0.0001, paired t-test, n = 20 cells). **(E)** Example traces of action potentials in the absence (control) and presence of 1 µM ML277. (F) Poincare plot showing the variability of the action potential duration to 90% repolarized (APD_{90}) in control and 1 µM ML277. **(G)** Mean APD_{90} in the absence (control), presence of 1 µM ML277 and washout in NT solution (***P<0.0001, Repeated-Measured ANOVA with Dunnett's post-test, n = 17 cells). **(H)** Mean calcium transient traces from 6 cardiomyocytes recorded using Fura-2, in the absence (control) and presence of 1 µM ML277. **(I)** Mean peak amplitude of calcium transients in the the absence (control) and presence of 1 µM ML277 measured as a change in Fura-2 ratio. Peak amplitude calculated as the mean peak from 10 transients after 5 minutes of perfusion with control solution and 5 minutes of perfusion with 1 µM ML277 (***P=0.0006, paired t-test, n = 34 cells). **(J)** Mean area under the curve analysis for cells in figure I (***P<0.0001, paired t-test, n = 34 cells).

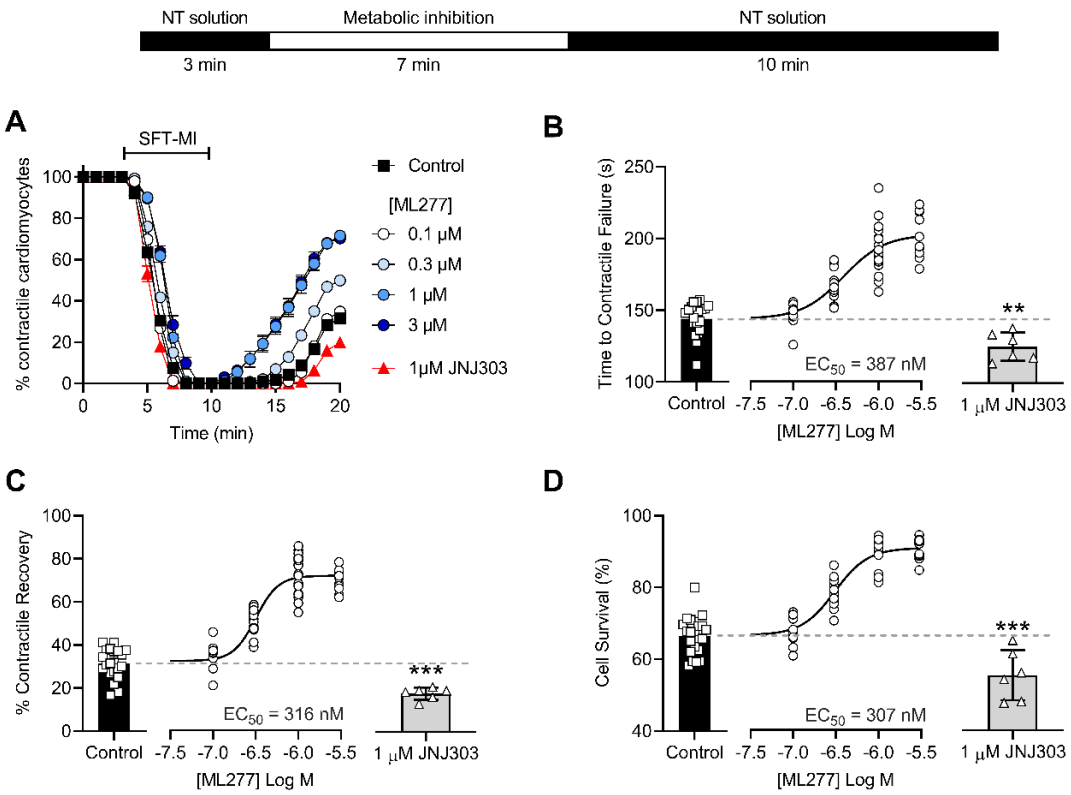

Figure 2: Perfusion of cardiomyoyctes with ML277 during a metabolic inhibition and washout protocol imparts cardioprotection.

(A) time course of contractile cardiomyoyctes durin the metabolic inhibition and washout protocol (outlined above) in control contitions, with 0.1 – 3 µM ML277, or with 1 µM JNJ303. **(B)** mean change I nthe time to contractile failure in the conditions outlined in **(A)**. Dotted line represents the mean value in control conditions. (**P=0.0029, unpaired t-test, JNJ303 (n = 6) vs control (n = 9)). **(C)** mean change in the percentage of contractile recovery in the conditions outlined in (A). dotted line represents the mean value in control conditions. (***P<0.0001, unpaired t-test, JNJ303 (n = 6) vs control (n = 9). **(D)** Data demonstrating the mean change I nthe percentage of cell survival in conditions outlined in (A). Dotted line represents the mean value in control consitions. (P=0.0008, unpaired t-test, JNJ303 (n = 6) vs control (n = 9 (288 cells)). For ML277 experiments, control (no drug) n = 21 (661 cells). For ML277, n = 12 (353), 14 (415), 18 (495 and 12 (408) experiments (cells) for 0.1, 0.3, 1 and 3 µM respectively. Calculated EC_{50} values are included in each figure panel for clarity.

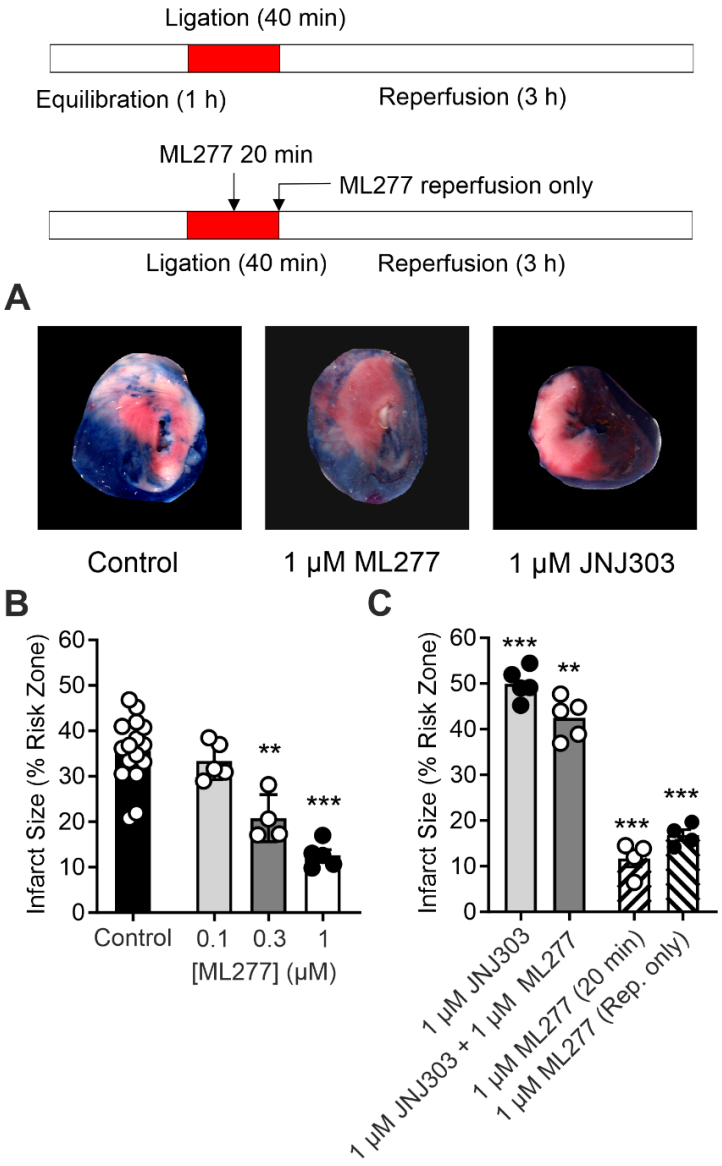

Figure 3: ML277 imparts cardioprotection to the whole heart in a *ex vivo* coronary ligation protocol.

Whole hearts were perfused in a retrograde manner via the aorta for 1 hour to acclimatise. The left anterior descending (LAD) coronary artery was ligated for 40 min, followed by reperfusion for 3 hours. **(A)** Example images from heart slices stained with Evans blue indicator, showing areas unaffected by the coronary ligation, and living or infarcted tissue as shown using 2,3,5-triphenyltetrazolium chloride (TTC) staining (red and white staining, respectively). The percentage infarct size was calculated as the proportion of white staining as a fraction of the red and white stained regions using Image J. **(B)** Bar chart showing the mean effects of 0.1 – 1 µM ML277 on infarct size when ML277 was included throughout the protocol. (**P=0.0002, ***P<0.0001, One-Way ANOVA with Dunnett's Post-test, n = 16, 5, 4 and 5 hearts for control, 0.1, 0.3 and 1 µM ML277 respectively). The mean area at risk (red + white stained) was not significantly different between groups (One-way ANOVA). **(C)** 1 µM JNJ303 in the absence or presence of 1 µM ML277 significantly increased infarct size (***P<0.0001, **P=0.0031, One-Way ANOVA with Dunnett's Post-test, n

= 16, 5 and 5 hearts for control, 1 µM JNJ303 and 1 µM JNJ303 with 1 µM ML277 respectively). 1 µM ML277 introduced to the perfusing solution 20 minutes into the ligation, or on reperfusion only significantly reduced the infarct size (***P<0.0001, One-Way ANOVA with Dunnett's Post-test, n = 16, 4 and 4 hearts for control, application at 20 min or on reperfusion respectively. There was no significant difference between the area at risk (One-Way ANOVA).

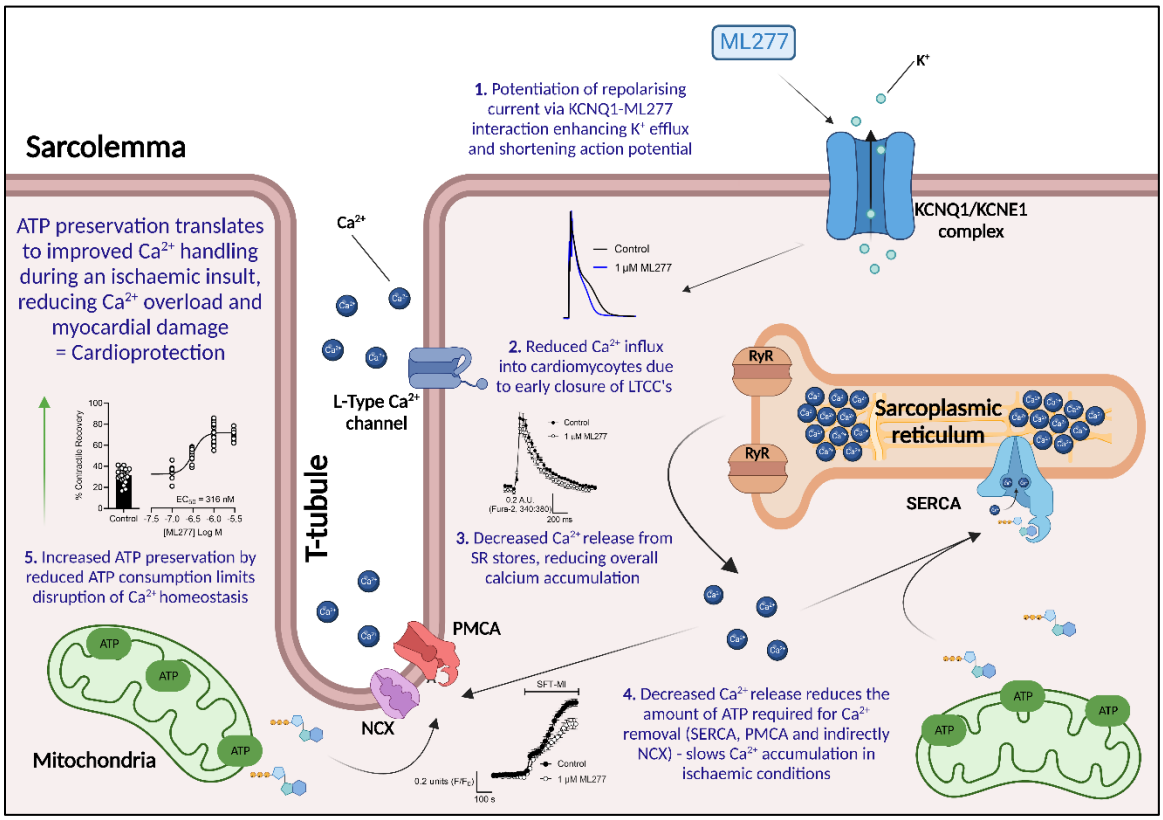

Figure 4:

Cartoon illustrating the mechanism by which IKs potentiation by ML277 imparts cardioprotection. Graphic created with BioRender.com.

Supporting Information for

IKs potentiation by ML277 is a novel cardioprotective intervention

Sean Brennan[1#], Abrar IM Alnaimi[1#], Lauren R McGuinness[1], Muhammad IM Abdelaziz[1], Robert A McKenzie[2], Sophie Draycott[2], Jacob Whitmore[1], Parveen Sharma[1], & Richard D Rainbow[1]*

Richard Rainbow

Email: richard.rainbow@liverpool.ac.uk

This PDF file includes:

Supporting text for methods

Figures S1 to S8

Supporting Information Text

Supplementary Methods

Isolation of ventricular myocytes.

The care and sacrifice of the animals conformed to the requirements of the UK Animals (Scientific Procedures) Act 1986 (2012 amendment). Ethical approval for all experimental procedures was granted by the University of Leicester/Liverpool's Animal Welfare and Ethical Review Body (AWERB_2018_44). Adult male Wistar rats (200 – 300 g), or Dunkin-Hartley guinea pigs (up to 500 g), were killed by Schedule 1 procedure of concussion and cervical dislocation. Following Schedule 1, the heart was quickly removed from the thoracic cavity and briefly submerged into cold (4°C) Ca^{2+}-free Tyrode's solution containing (in mM): KCl 5, NaCl 135, NaH_2PO_4 0.33, Na pyruvate 5, HEPES 10, Mannitol 15, Glucose 5, MgCl 1, EGTA 0.3, to halt contractions and to lower the metabolic demand. The isolated heart was then cannulated via the aorta and mounted on a Langendorff type apparatus and perfused in a retrograde manner with warmed Ca^{2+}-free Tyrode's solution (37°C) for 6 min. The enzyme mix solution (19 mg collagenase; 50 mg BSA prepared from factor V albumin and 16 mg protease; type XIV 15% Ca^{2+}, Sigma-Aldrich) was then perfused through the heart until isolated cells appeared in the perfusate sampled from the ventricles. The solution was then exchanged for Ca^{2+}-free Tyrode's solution for a further 2 min and then the heart cut down, washed in normal Tyrode's (NT) solution containing (in mM): KCl 5, NaCl 135, NaH_2PO_4 0.33, Na pyruvate 5, HEPES 10, Mannitol 15, Glucose 5, MgCl 1, $CaCl_2$ 2, and cardiomyocytes mechanically separated using a shaking water bath at 37°C. This technique yielded 70–90% rod-shaped cardiomyocytes, which were stored in NT solution at room temperature and used within 12 h of isolation.

HEK293 culture and transfection:

Human embryonic kidney 293 (HEK293) cells were transiently transfected using FuGENE®6 with KCNQ1 and KCNE1 cDNA in a 2:1 ratio. Both *KCNQ1* and *KCNE1* genes were cloned into a pIRES2-EGFP vector and so transfected cells were identified by their green fluorescence under 480 nm epifluorescent illumination. HEK293 cells were maintained in Dulbecco's Modified Eagle Medium (DMEM) containing 10% serum FBS and 1% penicillin / streptomycin.

HEK293 cells stably expressing hERG subunits were maintained in Dulbecco's Modified Eagle Medium (DMEM) containing 10% serum FBS (myoclone) and the selection antibiotics gentamycin and geneticin (G418).

Patch-clamp electrophysiology.

Patch electrodes were made from filamented thick-walled borosilicate glass with a resistance of 3-6 MΩ. Recordings were made from isolated cardiomyocytes using an Axopatch 200B amplifier, filtering at 2 kHz. Recordings were digitized using a Digidata 1440 and recorded and analyzed using pCLAMP 10.3 software (Axon Instruments, Scientifica, Uckfield UK).

Whole-cell: Intracellular electrode solution contained (in mM) 30 KOH, 110 KCl, 10 EGTA, 10 HEPES, 1 $MgCl_2$, 1 Mg-ATP, 0.1 Na-ADP, 0.1 GTP plus 20 nM $CaCl_2$, pH 7.2 with HCl.

Action potential (AP): In current-clamp mode, APs were stimulated at 1 Hz via the patch electrode with a 5-ms depolarizing trigger, set to 130% of that required to elicit an AP (approximately 500-900 pA). Action potential duration to 90% repolarized (APD_{90}) and membrane potential (Vm) were calculated within pCLAMP software offline (2, 17, 20).

Whole cell currents: In voltage-clamp mode, various protocols were used, these are shown in relevant figures in the results section (2, 17, 20). In all cases, one recording was made per cell.

Simulated ischemia and reperfusion model.

Freshly isolated ventricular cardiomyocytes were stimulated to contract using electric field stimulation (EFS) at 1 Hz. Contractile function was observed via a JVC CCTV camera and recorded to DVD for offline analysis. For simulated ischemia and reperfusion (I/R) experiments, cardiomyocytes were perfused (5 ml/min at 32-34°C) with NT solution for 2 min and substrate-free metabolic inhibition Tyrode's solution (SFT-MI; containing 2 mM cyanide and 1 mM iodoacetic acid) for 7 min, followed by 10 min of NT (reperfusion). Analysis was performed on the video file recordings to measure contractile and morphological changes of cardiomyocytes, such as contractile recovery after simulated ischemia, time to contractile failure and cell death (2, 17, 20).

Video-edge detection:

Cardiomyocytes were simulated to contract using 1 Hz EFS and contractile responses in the presence and absence of ML277 were recorded as outlined above. DVD recordings were played back and video-edge detection measurements were made using JVC CCTV camera connected through a Video-edge detection system (VED-105, Crescent electronics)/ The output was digitised using a Minidigi1B (Molecular Devices) and recorded to Axoscope 10.7 software (Molecular Devices). Area under the curve analysis was carried out using Graphpad Prism 9 on sequential contractions in the absence of, and following 5 minute of perfusion with, ML277. Mean data from 10 sequential contractions was used to create a single data point for each of the parameters

shown (duration of contraction, amplitude of contraction, area under the curve, and the rates from baseline to peak and from peak back to baseline).

Fluorescence imaging:

To record calcium transients, cardiomyocytes were loaded with 5 µM Fura-2-AM for 20 minutes at room temperature. Cells were stimulated to contract at 1 Hz using electric field stimulation (EFS) and perfused at 32°C. Data was acquired using Winfluor4.2 software (Strathclyde University), with 340 and 380 nm excitation illumination provided by a PTI DeltaRam X monochromator. Emissions were collected using Andor Zyla4.5 camera at wavelength greater than 520 nm. Images were acquired at a rate of 26 ratios per second.

For more detailed analysis of the Ca^{2+} transients, cells were loaded with 5 µM Fluo-4-AM for 20 minutes. Cells were stimulated at 1 Hz using EFS and perfused with NT solution in the absence and presence of ML277 for 5 minutes each. Transients were recorded for 1 min in each condition, to limit photobleaching, at a rate of 40 images per second. Area under the curve analysis was carried out using Graphpad Prism 9 on sequential transients in the absence of, and following 5 minute of perfusion with, ML277. Mean data from 10 sequential transients was used to create a single data point for each of the parameters shown (duration of transient, amplitude of transient, area under the curve, and the rates from baseline to peak and from peak back to baseline).

For simultaneous measurements of calcium and mitochondrial membrane potential, cells were loaded with both 5 µM Fluo-4-AM and 1 µM Tetramethylrhodamine methyl ester (TMRM). At this concentration, TMRM accumulates in the mitochondria and auto quenches the signal. On depolarization of the mitochondria, the TMRM dissipates into the cytoplasm and the fluorescence increases. Fluorescence was excited alternately at 480 and 540 nm to excite the Fluo-4 and TMRM once every 5 seconds. Cells were perfused at 32 °C with normal Tyrode's solution for 3 min followed by the metabolic inhibition Tyrode's solution for 7 min. Cells were quiescent throughout to reduce movement artefacts, given that these were single wavelength indicators.

Langendorff-perfused heart and coronary artery ligation.

Following Schedule 1 killing by concussion and cervical dislocation, hearts from adult male Wistar rats (300–400 g) were quickly removed and cannulated on a Langendorff apparatus and perfused retrogradely with warmed Ca^{2+}-free Tyrode's solution (37°C) for 1 hr to stabilize. The left anterior descending coronary artery was then ligated for 40 minutes to cause ischemia, by using 5-0 USP

braided silk suture and two pipette tips to form a reversible knot around the artery (17). The knot was then removed to start the 3 hour reperfusion phase with the suture remaining in place to allow for re-ligation. During all phases temperature was carefully maintained at 37°C by submerging the heart in NT solution using a heated water jacket. Evans Blue dye (1% in NT solution) and 2,3,5-triphenyltetrazolium chloride (Sigma Aldrich) were used to identify area at risk (AAR) and infarcted area (IA), respectively. To determine the AAR and IA, each slice was scanned on both sides and weighed. AAR and IA were calculated for each of the slices from the heart using ImageJ. The AAR, IA and unaffected area sizes from ImageJ were then used to calculate the percentage infarct of the AAR by weight (17).

Computer model of a human cardiac action potential:

The human action potential was modeled using the O'Hara-Rudy CiPA v1.0 (2017) model running in OpenCOR software (16). For control conditions, the model was not modified from the original O'Hara-Rudy CiPA v1.0 (2017) model. Using data established in our HEK293 study (Supplementary figure 1) showing an ~30 mV leftward shift in activation curve and an approximate doubling of current, the model was modified to include a 30 mV leftward shift and a doubling of conductance to model the effect of ML277 on the human action potential, IKs current and intracellular Ca^{2+}.

Equation 1: original steady-state activation gate (xs1ss) parameters where -11.6 mV is the mid-point of the activation curve with a slope factor of 8.932 mV

$$xs1ss = \frac{1}{1 + e^{\frac{-(Vm+11.6)}{8.932}}}$$

Equation 2: Modified activation parameters to include 30 mV shift in the activation curve

$$xs1ss = \frac{1}{1 + e^{\frac{-(Vm+11.6+30)}{8.932}}}$$

In the original model, xs2ss=xs1ss to represent the inactivation gate. Given that, equation one was used to represent xs2ss in the enhanced IKs model, given the assumption of no change in inactivation with ML277.

To simulate the steady-state, the model was run for 10 cycles and the data generated in the final cycle was used to plot the action potential, IKs current and intracellular calcium changes in Supplementary Figure 6.

Supplementary data

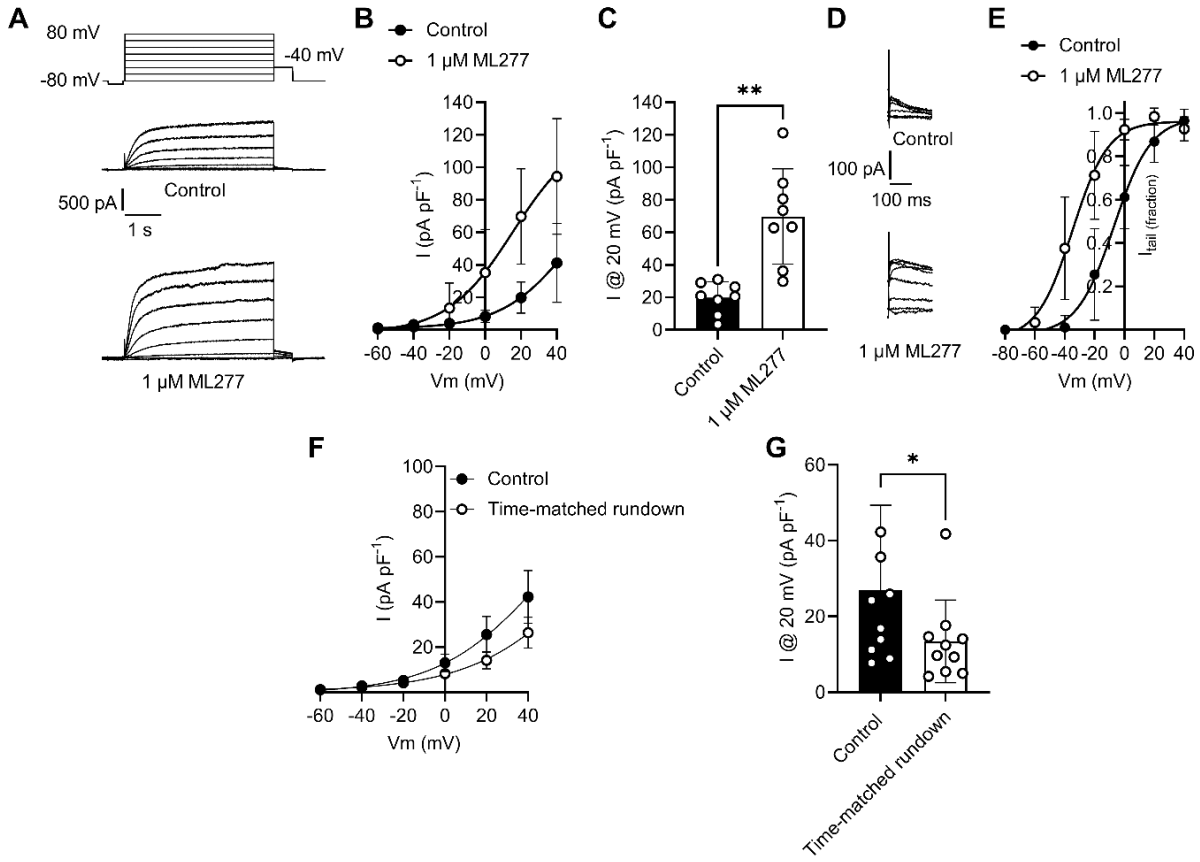

Figure S1

ML277 potentiates KCNQ1/KCNE1 current transiently expressed in HEK293 cells.

(A) Example current voltage relationship recordings from a HEK293 cell transiently transfected with KCNQ1/KCNE1 subunits in the absence and presence of 1 µM ML277. **(B)** Mean current-voltage relationship in the absence and presence of 1 µM ML277. **(C)** Mean whole-cell current density at 20 mV in the absence and presence of 1 µM ML277. (**P=0.0041, Paired t-test, n = 8). **(D)** Expanded tail currents from example traces in (A). **(E)** Mean activation curves plotted from the tail currents recorded at -40 mV with a half-maximal voltage of -6.9 ± 2.9 mV and -34.8 ± 3.4 mV in control and ML277 respectively. **(F)** Mean current-voltage relationship in control and time-matched rundown experiments in HEK293 cells **(G)** mean data at 20 mV showing the time matched rundown of KCNQ1/KCNE1 current (*P=0.0131, paired t-test, n = 9).

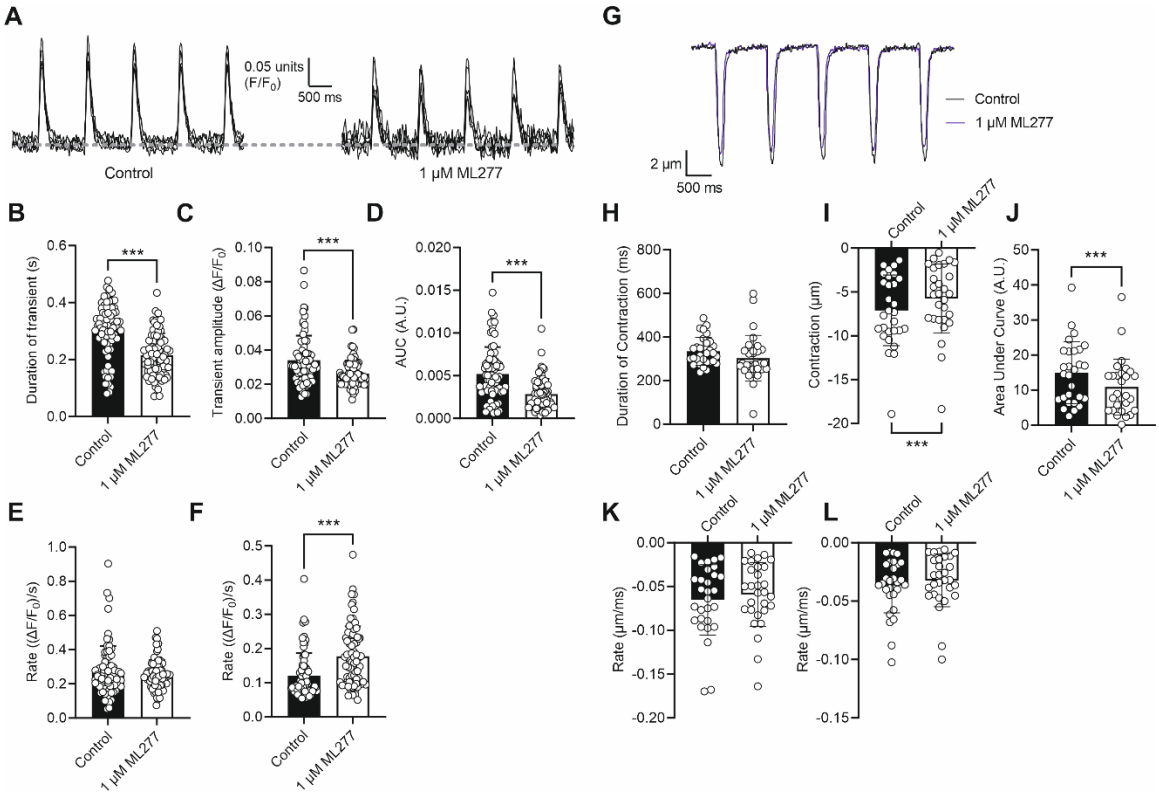

Figure S2

ML277 significantly alters the calcium transients, but has limited effects on cardiomyocyte contraction.

(A) Example calcium transients from 5 cells in the absence and presence of 1 µM ML277. **(B)** Mean duration, **(C)** mean amplitude, and **(D)** mean area under the curve for Ca^{2+} transients measured using Fluo-4, in 1 Hz electric field stimulation at 32 ± 2 °C, in the presence or absence of 1 µM ML277. **(E)** Mean rate from base to peak of the transient and **(F)** mean rate from peak to the return to the baseline. (***P<0.0001, Paired t-test, n = 75 cells from 5 experiments). **(G)** Example contractile responses from a single cardiomyocyte in the absence (black) and presence (blue) of 1 µM ML277. **(H)** Mean duration, **(I)** mean amplitude, and **(J)** mean area under the curve for contractions measured using video-edge detection, in 1 Hz electric field stimulation at 32 ± 2 °C, in the presence or absence of 1 µM ML277. **(K)** Mean rate from base to peak of the contraction and **(L)** mean rate from peak to the return to the baseline. (***P<0.0001, Paired t-test, n = 30 cells from 12 experiments).

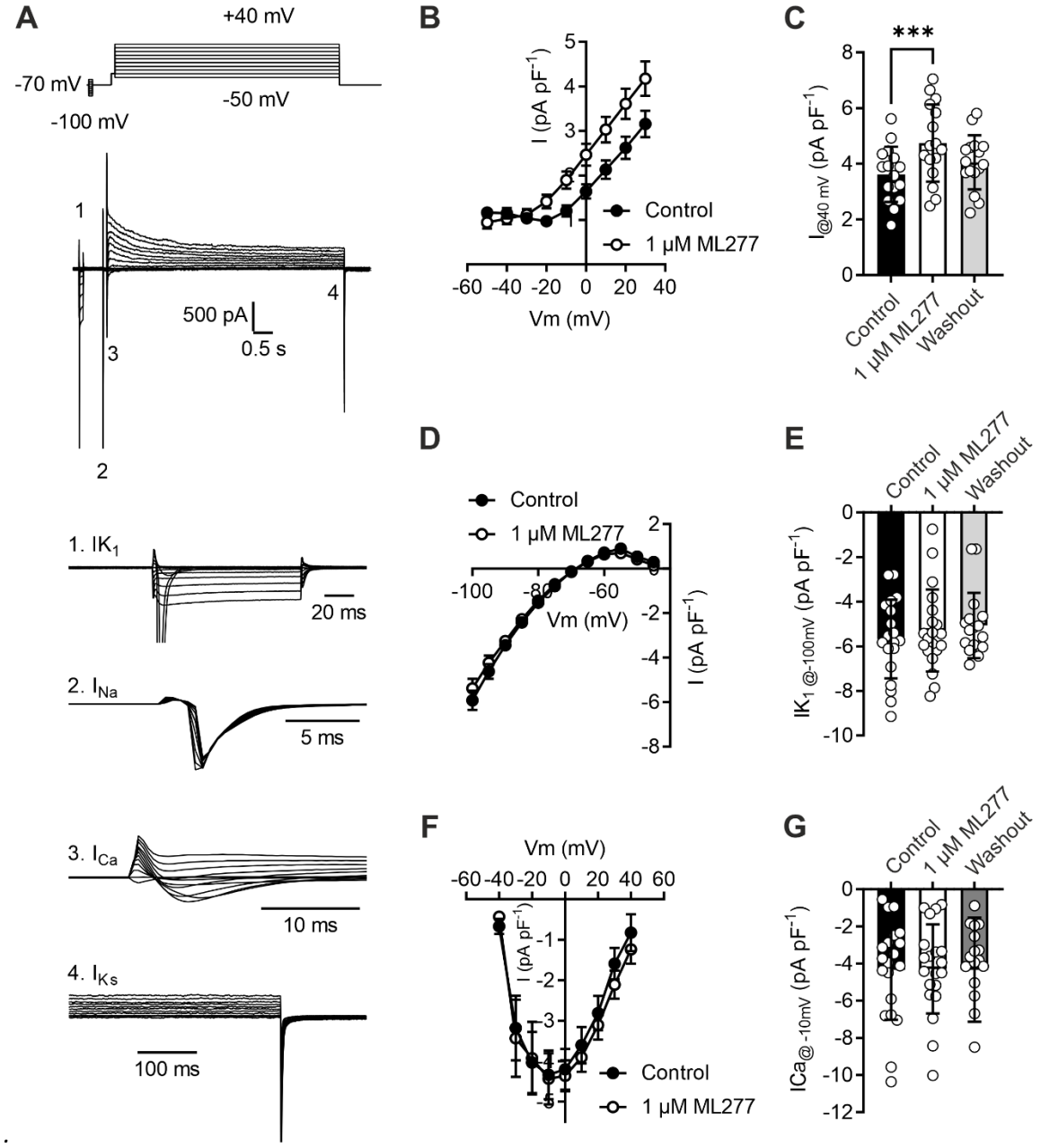

Figure S3

ML277 potentiates delayed rectifier currents in rat ventricular cardiomyocytes but does not affect IK_1 or calcium currents.

(A) Example traces of the protocol and expanded traces showing **1)** inward rectifier current (IK_1), **2)** Na currents (I_{Na}), **3)** Calcium currents (I_{Ca}) and **4)** Slowly activating K currents (I_{Ks}), in control conditions. **(B)** Mean current voltage relationship showing before and after 5 min of perfusion with 1 µM ML277. **(C)** Mean data showing the mean delayed rectifier current at the end of a 6 s depolarization to 40 mV. There was a significant increase in delayed rectifier current that was lost

following a 5 min washout of ML277 (**P<0.0001, Repeated-measures ANOVA with Dunnett's Post-test, n = 16 cells). **(D)** Mean current-voltage relationship for I_{K1} current before and following 5 min perfusion with 1 µM ML277 **(E)** Mean current at -100 mV showing no significant difference between control, 1 µM ML277 or washout (Repeated-measures ANOVA, n = 16 cells). **(F)** Mean current-voltage relationship for I_{Ca} current before and following 5 min perfusion with 1 µM ML277 **(G)** Mean current at -10 mV showing no significant difference between control, 1 µM ML277 or washout (Repeated-measures ANOVA, n = 16 cells).

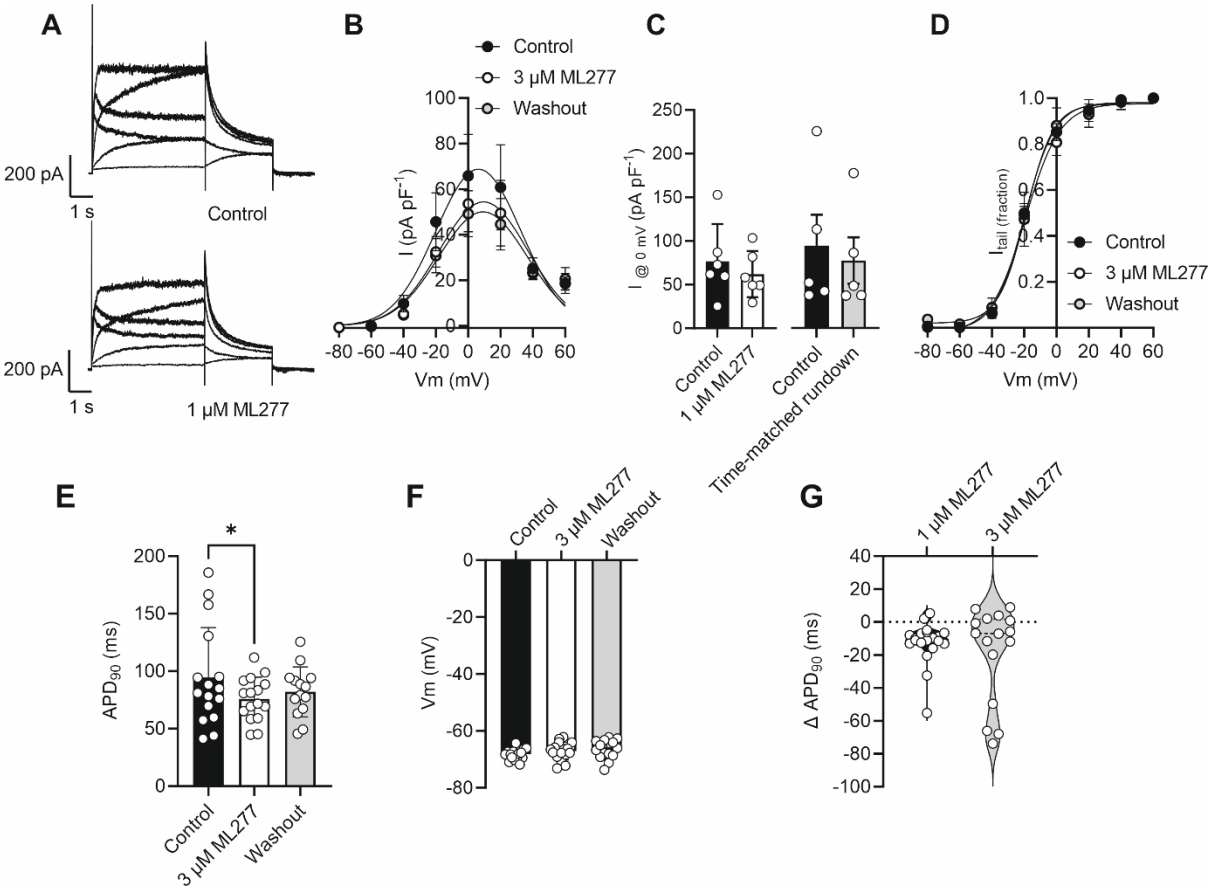

Figure S4

A supramaximal concentration of ML277 (3 µM) had no effect on hERG current stably expressed in HEK293 cells or any further shortening of the cardiac action potential duration.

(A) Example of a family of currents recorded from HEK293 cells stably expressing Kv11.1 and KCNE2 subunit. **(B)** Mean current voltage relationship from 6 cells showing control, 5 minutes of perfusion with 1 µM ML277 and following 5 minutes of washout. **(C)** Mean data from 1 µM ML277 treated, or time-matched rundown controls, showing no difference in the proportion of current rundown at 0 mV. **(D)** Mean tail current analysis showing no shift in the voltage-dependence of activation in control, 5 minute of perfusion with 1 µM ML277 and following 5 minute of washout. **(E)** Mean action potential duration in freshly isolated cardiomyocytes in control, 3 µM ML277 and washout solutions. **(F)** Mean membrane potential measurements for the same cells (*P=0.0370, Repeated Measures ANOVA with Dunnett's post-test, n = 16 cells). **(G)** Comparison of the change in APD_{90} on perfusion with ML277 at 1 and 3 µM. There was no significant difference between the groups (P=0.3996, Unpaired t-test, n = 20 and 16, for 1 and 3 µM ML277 respectively.

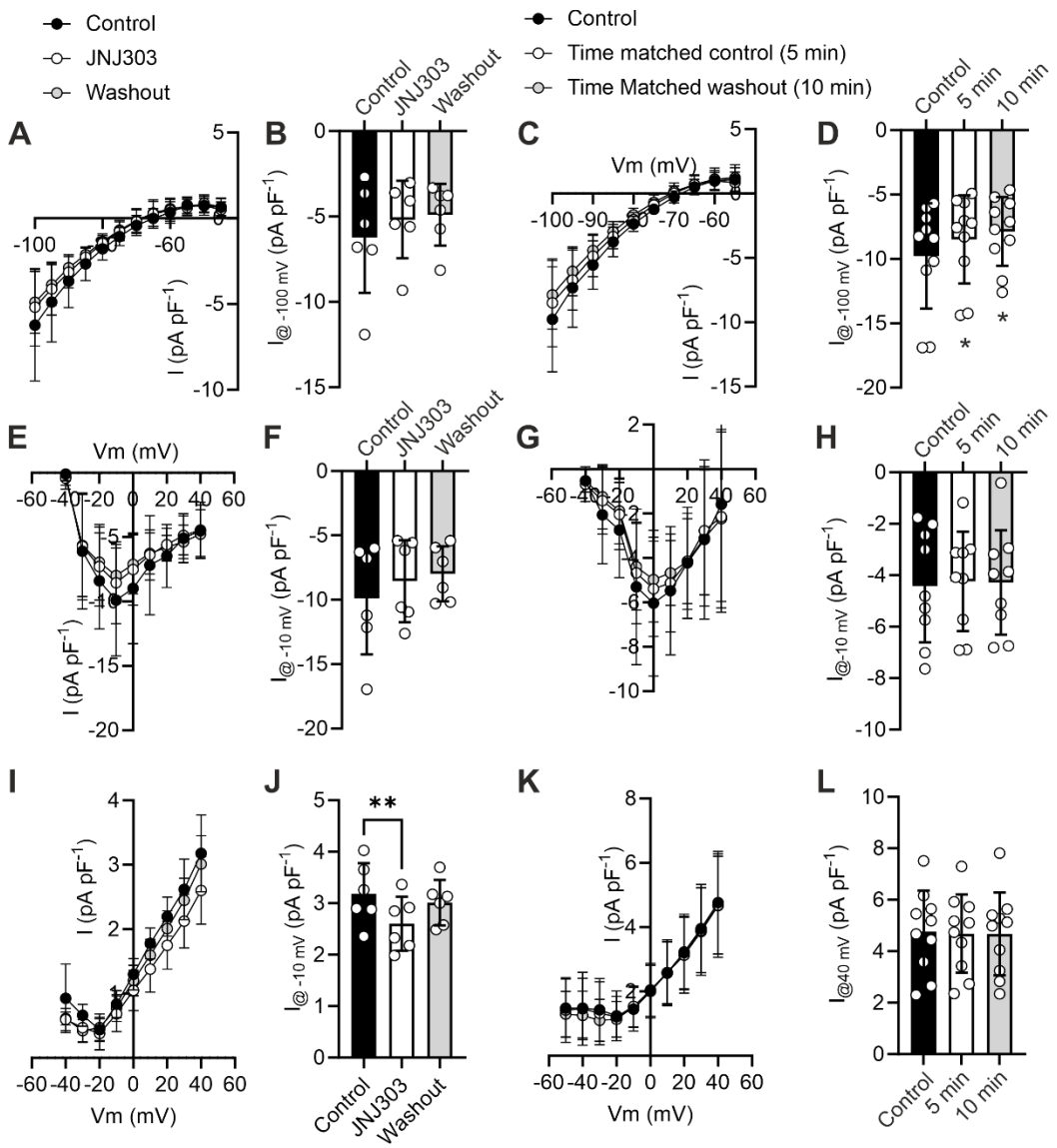

Figure S5

1 µM JNJ303 inhibits delayed rectifier currents in rat ventricular myocytes but does not cause more inhibition of other currents than run down.

All data recorded from an identical protocol as shown in Supplementary Figure 2 from rat isolated cardiomyocytes. **(A)** Mean current-voltage relationship for IK_1 currents recorded in control conditions, with 1 µM JNJ303, and following 5 min washout. **(B)** mean current density at -100 mV in the conditions in (A). (Repeated-measures ANOVA, 6 cells). **(C)** Mean current-voltage relationship for IK_1 currents recorded in control conditions, 5 min of perfusion as a time matched drug control and following 10 min of perfusion as a time-match for washout. **(D)** mean current density at -100 mV in the conditions in (C) (*P=0.045 and 0.041 for 5 and 10 min respectively, Repeated-measures ANOVA, 10 cells). **(E)** Mean current-voltage relationship for calcium currents

in the conditions outlined in (A). **(F)** mean current density at -10 mV as in the conditions outlined in (A). (Repeated-measures ANOVA with Dunnett's, 6 cells). **(G)** Mean current-voltage relationship for calcium currents in the conditions outlined in (C). **(H)** mean current density at -100 mV in the conditions in (C) (Repeated-measures ANOVA, 10 cells). **(I)** Mean current-voltage relationship for delayed rectifier currents in the conditions outlined in (A). **(J)** mean current density at 40 mV in the conditions outlined in (A). (**P=0.0064, Repeated-measures ANOVA with Dunnett's post-test, 6 cells). **(K)** Mean current-voltage relationship for delayed rectifier currents in the conditions outlined in (C). **(L)** mean current density at 40 mV in the conditions outlined in (C). (Repeated-measures ANOVA, 10 cells).

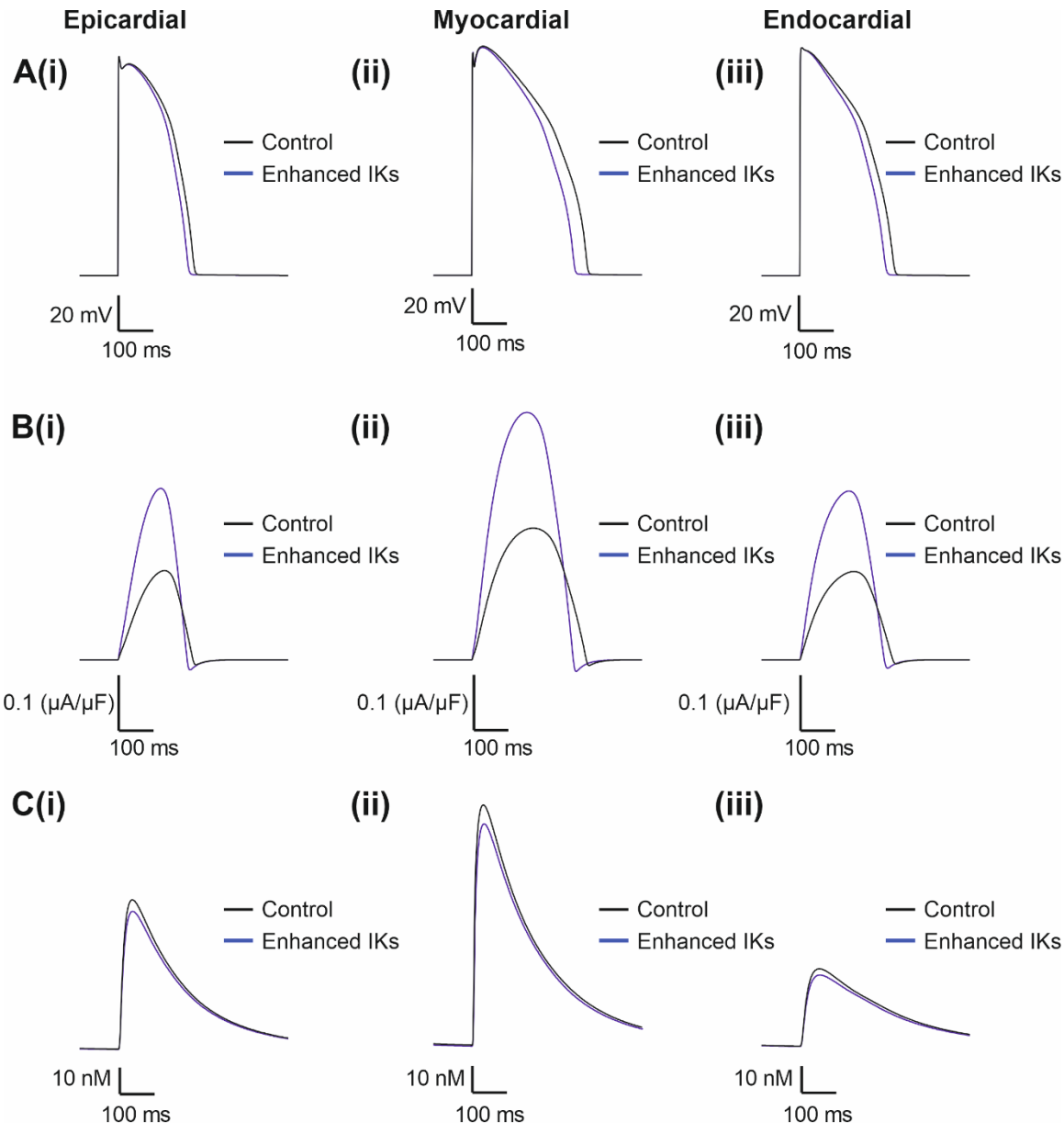

Figure S6

Computer simulation of the effects of enhanced IKs activity on the human cardiac action potential.

Responses in control conditions, and with IKs enhancement as seen using ML277, were modeled using the O'Hara-Rudy CiPA v1.0 (2017) model running in OpenCor software. Figures showing simulations of cardiac action potential **(A),** IKs current **(B)** and intracellular calcium change **(C)** in Epicardial (i), myocardial (ii) and endocardial myocytes in control conditions (unaltered model) and with enhanced IKs current. The enhancements to IKs were simulated by modifying the

equations from the computer model to match the parameters recorded in HEK293 cells transfected with KCNQ1/KCNE1, a 30 mV shift in activation curve and a doubling of current.

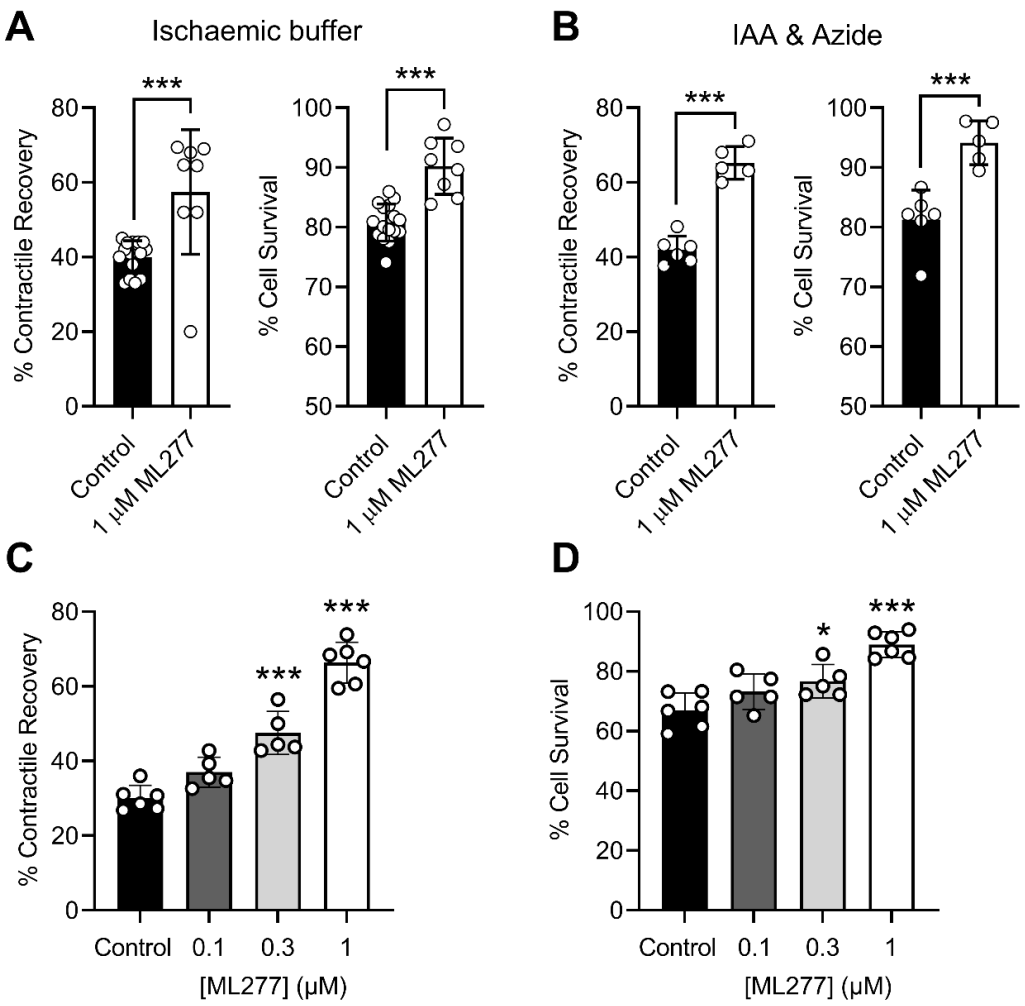

Figure S7

ML277 is protective in rat cardiomyocytes from two additional metabolic inhibition protocols and protective in guinea pig isolated cardiomyocytes

(A) Mean contractile recovery and cell survival data from an ischemic buffer protocol where the cells were treated with the ischemic buffer for 10 minutes, followed by 20 minutes washout. Similar to the data in figure 2, 1 μM ML277 imparted a significant cardioprotection, as evidenced by an increased contractile recovery and cell survival (***P=0.0006 and <0.0001, unpaired t-test, n = 16 (511 cells) and 8 (301 cells) control and ML277 respectively). **(B)** Mean contractile recovery and cell survival data from a substrate-free Tyrode's solution containing 1 mM iodoacetic acid and 20 mM sodium azide. The metabolic inhibition was applied for 10 minutes followed by a 20 min washout. Again, 1 μM ML277 imparted a significant cardioprotection, as evidenced by an increased contractile recovery and cell survival (***P<0.0001 and P=0.001, unpaired t-test, n = 6 (224 cells) and 5 (196 cells) control and ML277 respectively). Guinea pig cardiomyocytes were

exposed to the same protocol as outlined in Figure 2, demonstrating an ML277 concentration-dependent increase in **(C)** contractile recovery and **(D)** cell survival. (*P=0.0226, ***P<0.0001, One-Way ANOVA with Dunnett's post-test, n = 6 (180), 5 (142), 5 (110), 6 (145) experiments (cells) for control, 0.1, 0.3 and 1 μM ML277 respectively).

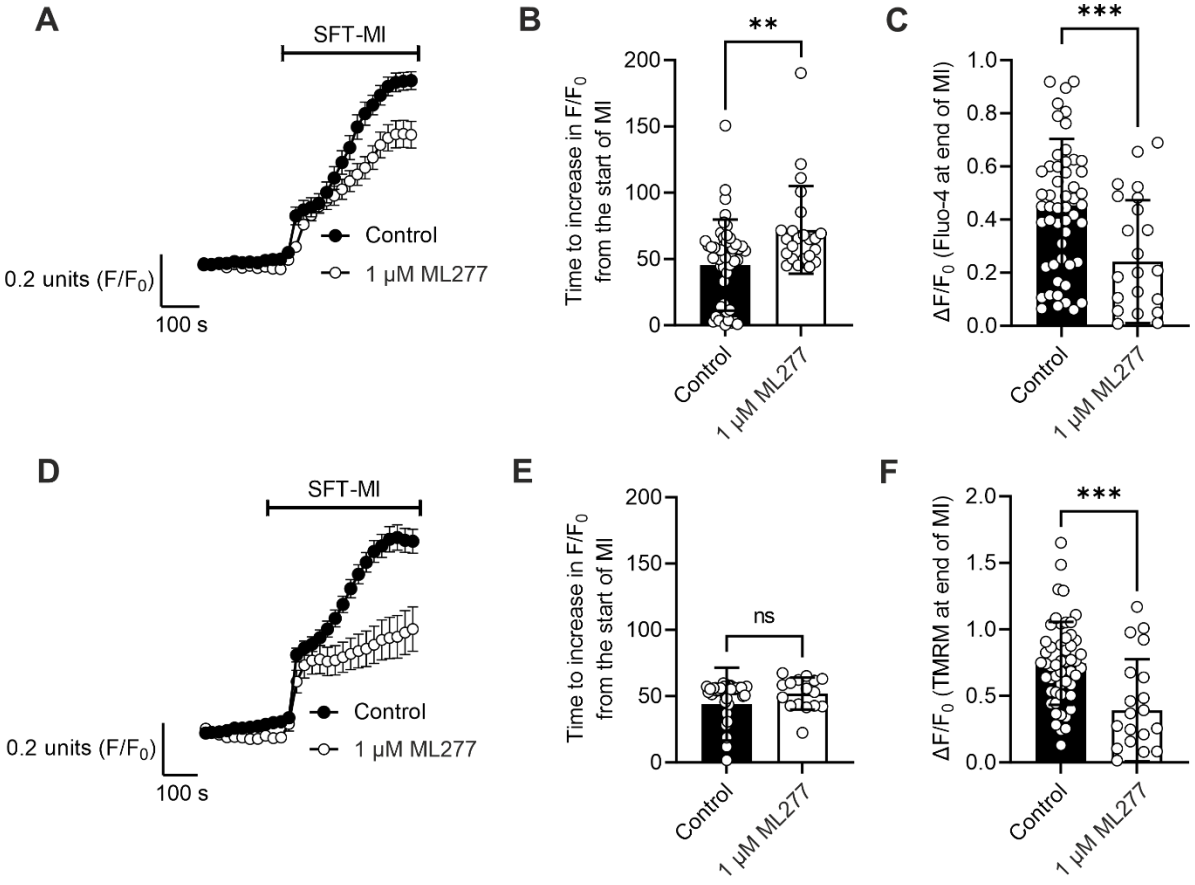

Figure S8

Calcium accumulation and mitochondrial depolarization are altered with ML277 treatment in a metabolic inhibition and washout protocol.

(A) Example time course data of the Fluo-4 signal from rat cardiomyocytes in the presence and absence of 1 µM ML277 in a metabolic inhibition and washout protocol. **(B)** Mean data showing the time to an increase of 10% above basal fluorescence in control and 1 µM ML277-treated cardiomyocytes (**P=0.0024, unpaired t-test, n = 53 control and 23 ML277 treated cells). **(C)** Mean data showing the change in Fluo-4 fluorescence from baseline at the end of the metabolic inhibition (***P=0.0007, unpaired t-test, n = 53 and 23, control and ML277 treated cells respectively). **(D)** Example time course data of the TMRM signal from the same rat cardiomyocytes as in (A) in the presence and absence of 1 µM ML277 in a metabolic inhibition and washout protocol. **(E)** Mean data showing the time to an increase of 10% above basal fluorescence in control and 1 µM ML277-treated cardiomyocytes (no significant difference unpaired t-test, n = 53 control and 23 ML277 treated cells). **(F)** Mean data showing the change in TMRM fluorescence from baseline at the end of the metabolic inhibition (***P=0.0001, unpaired t-test, n = 53 and 23 , control and ML277 treated cells respectively).

References:

1. C. E. Murry, R. B. Jennings, K. A. Reimer, Preconditioning with ischemia: a delay of lethal cell injury in ischemic myocardium. *Circulation* **74**, 1124-1136 (1986).
2. S. Brennan *et al.*, Early opening of sarcolemmal ATP-sensitive potassium channels is not a key step in PKC-mediated cardioprotection. *J Mol Cell Cardiol* **79**, 42-53 (2015).
3. C. Ozcan, M. Palmeri, T. L. Horvath, K. S. Russell, R. R. Russell, 3rd, Role of uncoupling protein 3 in ischemia-reperfusion injury, arrhythmias, and preconditioning. *Am J Physiol Heart Circ Physiol* **304**, H1192-1200 (2013).
4. R. M. Fryer, J. T. Eells, A. K. Hsu, M. M. Henry, G. J. Gross, Ischemic preconditioning in rats: role of mitochondrial K(ATP) channel in preservation of mitochondrial function. *Am J Physiol Heart Circ Physiol* **278**, H305-312 (2000).
5. H. E. Turrell, C. Thaitirarot, H. Crumbie, G. Rodrigo, Remote ischemic preconditioning of cardiomyocytes inhibits the mitochondrial permeability transition pore independently of reduced calcium-loading or sarcKATP channel activation. *Physiol Rep* **2** (2014).
6. L. Lu *et al.*, Metformin prevents ischaemic ventricular fibrillation in metabolically normal pigs. *Diabetologia* **60**, 1550-1558 (2017).
7. R. Macianskiene *et al.*, Mechanism of Action Potential Prolongation During Metabolic Inhibition in the Whole Rabbit Heart. *Front Physiol* **9**, 1077 (2018).
8. L. D. Plant, D. Xiong, H. Dai, S. A. Goldstein, Individual IKs channels at the surface of mammalian cells contain two KCNE1 accessory subunits. *Proc Natl Acad Sci U S A* **111**, E1438-1446 (2014).
9. X. Wu, H. P. Larsson, Insights into Cardiac IKs (KCNQ1/KCNE1) Channels Regulation. *Int J Mol Sci* **21** (2020).
10. M. E. Mattmann *et al.*, Identification of (R)-N-(4-(4-methoxyphenyl)thiazol-2-yl)-1-tosylpiperidine-2-carboxamide, ML277, as a novel, potent and selective K(v)7.1 (KCNQ1) potassium channel activator. *Bioorg Med Chem Lett* **22**, 5936-5941 (2012).
11. K. Willegems *et al.*, Structural and electrophysiological basis for the modulation of KCNQ1 channel currents by ML277. *Nat Commun* **13**, 3760 (2022).
12. H. Yu *et al.*, Dynamic subunit stoichiometry confers a progressive continuum of pharmacological sensitivity by KCNQ potassium channels. *Proc Natl Acad Sci U S A* **110**, 8732-8737 (2013).
13. Y. Xu *et al.*, Probing binding sites and mechanisms of action of an I(Ks) activator by computations and experiments. *Biophys J* **108**, 62-75 (2015).
14. G. Kanaporis, Z. M. Kalik, L. A. Blatter, Action potential shortening rescues atrial calcium alternans. *J Physiol* **597**, 723-740 (2019).
15. D. Ma *et al.*, Characterization of a novel KCNQ1 mutation for type 1 long QT syndrome and assessment of the therapeutic potential of a novel IKs activator using patient-specific induced pluripotent stem cell-derived cardiomyocytes. *Stem Cell Res Ther* **6**, 39 (2015).
16. S. Dutta *et al.*, Optimization of an In silico Cardiac Cell Model for Proarrhythmia Risk Assessment. *Front Physiol* **8**, 616 (2017).
17. S. Brennan *et al.*, A novel form of glycolytic metabolism-dependent cardioprotection revealed by PKCalpha and beta inhibition. *J Physiol* **597**, 4481-4501 (2019).
18. C. L. Lawrence, R. D. Rainbow, N. W. Davies, N. B. Standen, Effect of metabolic inhibition on glimepiride block of native and cloned cardiac sarcolemmal K(ATP) channels. *Br J Pharmacol* **136**, 746-752 (2002).

19. R. D. Rainbow *et al.*, SUR2A C-terminal fragments reduce KATP currents and ischaemic tolerance of rat cardiac myocytes. *J Physiol* **557**, 785-794 (2004).
20. M. W. Sims *et al.*, PKC-mediated toxicity of elevated glucose concentration on cardiomyocyte function. *Am J Physiol Heart Circ Physiol* **307**, H587-597 (2014).
21. D. Hudman, N. B. Standen, Protection from the effects of metabolic inhibition and reperfusion in contracting isolated ventricular myocytes via protein kinase C activation. *J Mol Cell Cardiol* **37**, 579-591 (2004).
22. C. L. Lawrence, B. Billups, G. C. Rodrigo, N. B. Standen, The KATP channel opener diazoxide protects cardiac myocytes during metabolic inhibition without causing mitochondrial depolarization or flavoprotein oxidation. *Br J Pharmacol* **134**, 535-542 (2001).
23. G. C. Rodrigo, N. W. Davies, N. B. Standen, Diazoxide causes early activation of cardiac sarcolemmal KATP channels during metabolic inhibition by an indirect mechanism. *Cardiovasc Res* **61**, 570-579 (2004).
24. G. C. Rodrigo, C. L. Lawrence, N. B. Standen, Dinitrophenol pretreatment of rat ventricular myocytes protects against damage by metabolic inhibition and reperfusion. *J Mol Cell Cardiol* **34**, 555-569 (2002).
25. G. C. Rodrigo, N. J. Samani, Ischemic preconditioning of the whole heart confers protection on subsequently isolated ventricular myocytes. *Am J Physiol Heart Circ Physiol* **294**, H524-531 (2008).
26. G. C. Rodrigo, N. B. Standen, Role of mitochondrial re-energization and Ca2+ influx in reperfusion injury of metabolically inhibited cardiac myocytes. *Cardiovasc Res* **67**, 291-300 (2005).
27. H. E. Turrell, G. C. Rodrigo, R. I. Norman, M. Dickens, N. B. Standen, Phenylephrine preconditioning involves modulation of cardiac sarcolemmal K(ATP) current by PKC delta, AMPK and p38 MAPK. *J Mol Cell Cardiol* **51**, 370-380 (2011).
28. E. Wrobel *et al.*, KCNE1 induces fenestration in the Kv7.1/KCNE1 channel complex that allows for highly specific pharmacological targeting. *Nat Commun* **7**, 12795 (2016).
29. X. Guo *et al.*, IKs protects from ventricular arrhythmia during cardiac ischemia and reperfusion in rabbits by preserving the repolarization reserve. *PLoS One* **7**, e31545 (2012).
30. J. Hansen *et al.*, Impact of Administration Time and Kv7 Subchannels on the Cardioprotective Efficacy of Kv7 Channel Inhibition. *Drug Des Devel Ther* **14**, 2549-2560 (2020).
31. K. K. Corydon *et al.*, Effect of ischemic preconditioning and a Kv7 channel blocker on cardiac ischemia-reperfusion injury in rats. *Eur J Pharmacol* **866**, 172820 (2020).
32. H. S. Wang *et al.*, KCNQ2 and KCNQ3 potassium channel subunits: molecular correlates of the M-channel. *Science* **282**, 1890-1893 (1998).
33. H. S. Wang, B. S. Brown, D. McKinnon, I. S. Cohen, Molecular basis for differential sensitivity of KCNQ and I(Ks) channels to the cognitive enhancer XE991. *Mol Pharmacol* **57**, 1218-1223 (2000).
34. C. E. Molina, J. Heijman, D. Dobrev, Differences in Left Versus Right Ventricular Electrophysiological Properties in Cardiac Dysfunction and Arrhythmogenesis. *Arrhythm Electrophysiol Rev* **5**, 14-19 (2016).
35. L. Z. Yu H, Xu K, Huang X, Long S, Wu M, McManus OB, Le Engers J, Mattmann ME, Engers DW, Le UM, Lindsley CW, Hopkins CR, Li M., Identification of a novel, small

molecule activator of KCNQ1 channels. *Probe Reports from the NIH Molecular Libraries Program [Internet].* (2011).
36. R. Towart *et al.*, Blockade of the I(Ks) potassium channel: an overlooked cardiovascular liability in drug safety screening? *J Pharmacol Toxicol Methods* **60**, 1-10 (2009).
37. C. Moreno *et al.*, A new KCNQ1 mutation at the S5 segment that impairs its association with KCNE1 is responsible for short QT syndrome. *Cardiovasc Res* **107**, 613-623 (2015).
38. Y. H. Chen *et al.*, KCNQ1 gain-of-function mutation in familial atrial fibrillation. *Science* **299**, 251-254 (2003).
39. D. J. Hausenloy, D. M. Yellon, Reperfusion injury salvage kinase signalling: taking a RISK for cardioprotection. *Heart Fail Rev* **12**, 217-234 (2007).
40. D. J. Hausenloy, D. M. Yellon, Preconditioning and postconditioning: united at reperfusion. *Pharmacol Ther* **116**, 173-191 (2007).
41. D. J. Hausenloy, A. Tsang, D. M. Yellon, The reperfusion injury salvage kinase pathway: a common target for both ischemic preconditioning and postconditioning. *Trends Cardiovasc Med* **15**, 69-75 (2005).
42. X. Rossello, D. M. Yellon, The RISK pathway and beyond. *Basic Res Cardiol* **113**, 2 (2018).
43. G. R. Budas, D. Mochly-Rosen, Mitochondrial protein kinase Cepsilon (PKCepsilon): emerging role in cardiac protection from ischaemic damage. *Biochem Soc Trans* **35**, 1052-1054 (2007).
44. N. Duquesnes, F. Lezoualc'h, B. Crozatier, PKC-delta and PKC-epsilon: foes of the same family or strangers? *J Mol Cell Cardiol* **51**, 665-673 (2011).
45. T. Miura, HASF, a PKC-epsilon activator with novel features for cardiomyocyte protection. *J Mol Cell Cardiol* **69**, 1-3 (2014).
46. M. V. Cohen, C. P. Baines, J. M. Downey, Ischemic preconditioning: from adenosine receptor to KATP channel. *Annu Rev Physiol* **62**, 79-109 (2000).
47. A. Dana, G. F. Baxter, D. M. Yellon, Delayed or second window preconditioning induced by adenosine A1 receptor activation is independent of early generation of nitric oxide or late induction of inducible nitric oxide synthase. *J Cardiovasc Pharmacol* **38**, 278-287 (2001).
48. T. Minamino, Cardioprotection from ischemia/reperfusion injury: basic and translational research. *Circ J* **76**, 1074-1082 (2012).
49. J. M. Downey, A. M. Davis, M. V. Cohen, Signaling pathways in ischemic preconditioning. *Heart Fail Rev* **12**, 181-188 (2007).
50. P. K. Randhawa, A. S. Jaggi, Opioids in Remote Ischemic Preconditioning-Induced Cardioprotection. *J Cardiovasc Pharmacol Ther* **22**, 112-121 (2017).